Title: Refractory for Black Liquor Gasifiers

Type of Report: Quarterly Report

Reporting Period Start Date: October 1, 2002

Reporting Period End Date: June 30, 2003

Principal Authors: William L. Headrick Jr. and Alireza Rezaie

Date Report Issued: August 2003

DOE Award Number: DE-FC26-02NT41491

Name and Address of Submitting Organization:
Curators of the University of Missouri on behalf of University of Missouri-Rolla
Sponsored Programs
1870 Miner Circle
215 ME Annex
Rolla, MO 65409-1330

DISCLAIMER

ABSTRACT

The University of Missouri-Rolla will identify materials that will permit the safe, reliable and economical operation of combined cycle gasifiers by the pulp and paper industry. The primary emphasis of this project will be to resolve the materials problems encountered during the operation of low-pressure high-temperature (LFHT) and low-pressure low-temperature (LPLT) gasifiers while simultaneously understanding the materials barriers to the successful demonstration of high-pressure high-temperature (HPHT) black liquor gasifiers. This study will define the chemical, thermal and physical conditions in current and proposed gasifier designs and then modify existing materials and develop new materials to successfully meet the formidable material challenges. Resolving the material challenges of black liquor gasification combined cycle technology will provide energy, environmental, and economic benefits that include higher thermal efficiencies, up to three times greater electrical output per unit of fuel, and lower emissions. In the near term, adoption of this technology will allow the pulp and paper industry greater capital effectiveness and flexibility, as gasifiers are added to increase mill capacity. In the long term, combined-cycle gasification will lessen the industry's environmental impact while increasing its potential for energy production, allowing the production of all the mill's heat and power needs along with surplus electricity being returned to the grid. An added benefit will be the potential elimination of the possibility of smelt-water explosions, which constitute an important safety concern wherever conventional Tomlinson recovery boilers are operated.

Developing cost-effective materials with improved performance in gasifier environments may be the best answer to the material challenges presented by black liquor gasification. Refractory materials may be selected/developed that either react with the gasifier environment to form protective surfaces in-situ; are functionally-graded to give the best combination of thermal, mechanical, and physical properties and chemical stability; or are relatively inexpensive, reliable repair materials. Material development will be divided into 2 tasks:

Task 1, Development and property determinations of improved and existing refractory systems for black liquor containment. Refractory systems of interest include magnesia aluminate and baria aluminate spinels for binder materials, both dry and hydratable, and materials with high alumina contents, 85-95 wt%, aluminum oxide, 5.0-15.0 wt%, and BaO, SrO, CaO, ZrO and SiC.

Task 2, Finite element analysis of heat flow and thermal stress/strain in the refractory lining and steel shell of existing and proposed vessel designs. Stress and strain due to thermal and chemical expansion has been observed to be detrimental to the lifespan of existing black liquor gasifiers. The thermal and chemical strain as well as corrosion rates must be accounted for in order to predict the lifetime of the gasifier containment materials.

TABLE OF CONTENTS

LIST OF GRAPHICAL MATERIALS

INTRODUCTION

Papermaking by the kraft process involves treatment of wood chips in a digester vessel with a steam-sodium sulfide-sodium hydroxide mixture to separate the cellulose fibers from the lignin that binds them together. The streams exiting the digester vessel include a fiber-rich stream that is further treated to provide the fibers that are used to form paper or other cellulose-based products. The other stream is identified as black liquor which is an aqueous solution containing the waste organic material including the lignin as well as the spent pulping chemicals that are primarily sodium carbonate and sodium sulfate. Black liquor (BL), a by-product of the papermaking process, is an important liquid fuel in the pulp and paper industry [1]. A diagram highlighting the steps in papermaking and chemical recovery is shown in Figure 1.

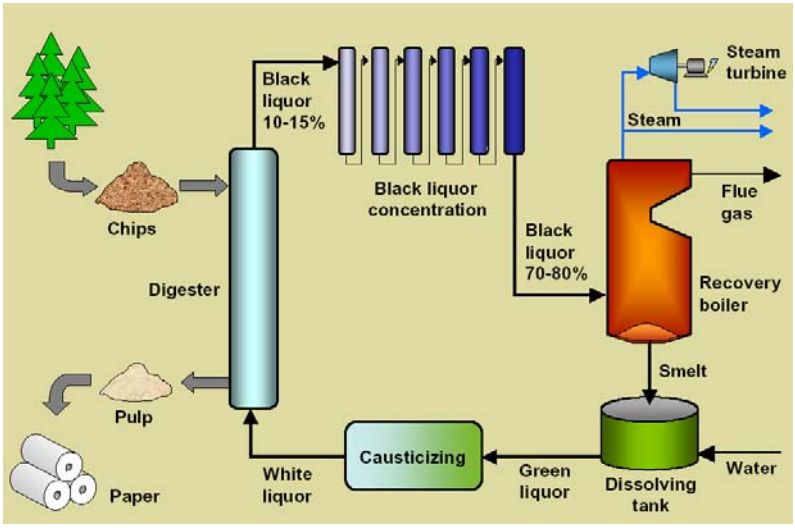

Figure 1 Schematic description of the pulping process [2]

The weak black liquor has a solids content of approximately 15% by weight but the strong black liquor resulting from the concentrator has a solids content of around 75%.[1] Black liquor represents a readily available renewable energy source which is expected to become an increasingly important resource for power generation in the pulp and paper industry in the future[3].

As is seen in Figure 2, the worldwide black liquor production is increasing. Moreover, the contribution of the United States to this rate is disproportionately high which shows the huge amount of energy and electricity power which can be obtained from black liquor by 2025[4]. Therefore development of a refractory lining material resistant to harsh condition of black liquor gasifier is necessary to provide a stable operating condition. The most readily apparent feature of gasification based power plants compared to existing power plants is the much higher levels of electricity production resulting from the high efficiencies of gas turbine cycles compared to those of steam turbines [5]. The following electrical power yields are rough estimates; 500-800 kWh/ADMT[1] for recovery boiler

[1] ADMT=Air Dried per Metric Ton

technology and 1200-1800 kWh/ADMT for pressurized black liquor gasification with combined cycle technology [6].

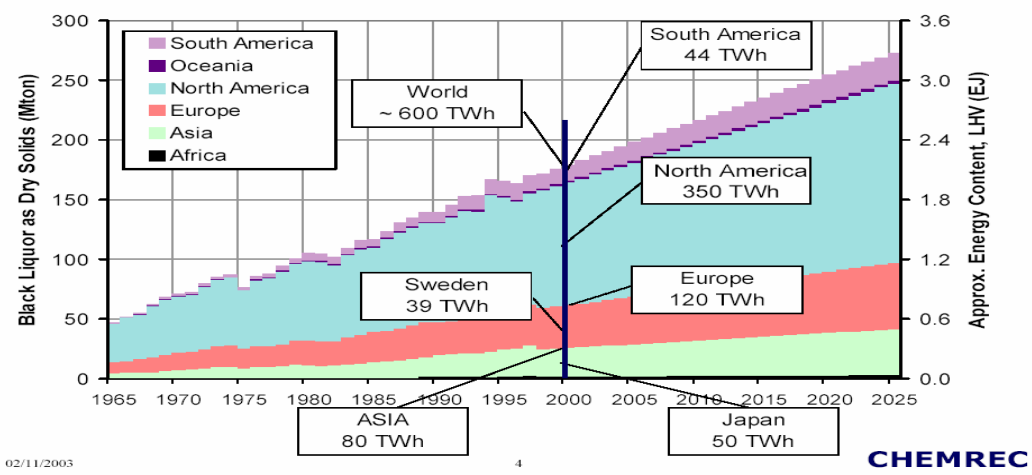

Figure 2 Estimated black liquor production (World) [4]

Moreover, Figure 3 shows the potential for electricity production from Black Liquor in Sweden. Of course the same trend should exist in the other countries of the world such as the United States. Again the importance of the role of Black Liquor Gasification as a future source of energy is obvious in this figure so attempts to further develop this process are warranted [4].

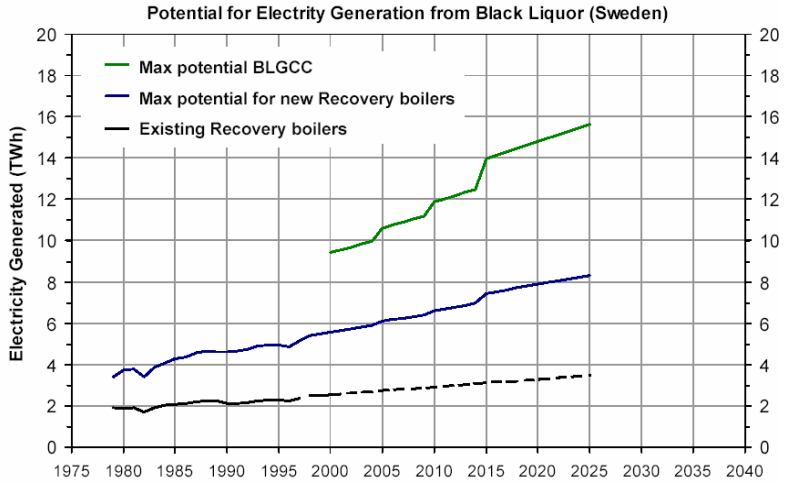

Figure 3 Maximum electric power Potential from black liquor [4]

In a very simple way in gasification process, the carbon in the dry solids reacts with steam which is formed when the black liquor is heated in the reactor [6].

$$C + H_2O \longrightarrow CO + H_2 \qquad (1)$$

This is an endothermic reaction, which requires a temperature of $1650-1830^{\circ}F (900-1000^{\circ}C)$ in order to proceed rapidly. In the gasification process, an exothermal reaction is used to raise the temperature to the required level and generate the heat needed to support the reaction shown above. This exothermal reaction is combustion (oxidation) of carbon to carbon dioxide [6].

$$C + O_2 \longrightarrow CO_2 \qquad (2)$$

Adding the above two reaction gives:

$$2C + H_2O + O_2 \longrightarrow CO + CO_2 + H_2 \qquad (3)$$

Very simplified, the black liquor is partially burned and partially gasified [6].

Black liquor gasification (BLG) is a process wherein black liquor is partially burned with a substoichiometric amount of air or oxygen to recover process chemicals and convert the organic portion of the liquor into a usable fuel gas [7]. Boilers and gasifiers are the two main equipment types used to convert some of the chemical energy of black liquor by combustion of the liquor which yields an inorganic smelt and gases. The old method to regenerate the pulping chemicals as well as recover some of the heating value contained in the organic components was the black liquor recovery boiler. Concentrated black liquor is injected into this boiler where the water is evaporated, organic materials are burned to produce heat and steam, and inorganic components are recovered in the bottom of the boiler in a partially reduced state, primarily as sodium carbonate and sodium sulfate. [8]

Recovery boilers have been used successfully for many years but they have a number of shortcomings. First, the boiler is the most expensive piece of capital equipment in a typical kraft pulp mill. Second, the boiler is not efficient for recovering energy from black liquor and producing electric power. Besides, there is a safety issue because of the potential for recovery boiler explosions if the pressurized water contained in the tubes leaks and contacts the bed of molten smelt. Contact of this hot water with the molten smelt can result in violent explosions [7, 8]. The pulp and paper industry is interested in increasing the chemical recovery process efficiency, either by improving recovery boiler performance or by implementing alternative technologies. The development and selection of recovery equipment during the next two decades will be affected by: [7]

- Aging recovery equipment
- Need for incremental pulp production capacity
- Changes in mill energy demand, i.e. more electricity and less stream
- More stringent emissions regulations

It is reported that the net power output per ton of pulp is 40.7 MW in recovery boiler and 78.4 MW in CHEMREC BL gasifier. Also it is reported that the overall thermal efficiency is 67.5% in recovery boiler and 77.5% in CHEMREC BL gasifier [6].

Black liquor gasification (BLG) is widely viewed as the technology most likely to replace the recovery boiler. Gasification is the conversion of low-cost solids (like biomass) or liquids (like black liquor) into clean-burning gases (usually for replacement of fossil fuels) [10]. Combined cycle denotes the use of a gaseous fuel in a gas turbine followed by the production of steam, which is subsequently used in a steam turbine such that both turbines produce electric power. Splitting sulfur and sodium present in the recovered pulping chemicals into separate process streams is the other advantage of the BLG process. This opens up the opportunity to produce a wide range of pulping liquor compositions [6, 7, 11].

The temperature level defines whether the technology operates below or above the melting point of the smelt produced [9, 10]. Among different gasification processes, only two of them have had satisfactory results and are still in operation. The first one is the low temperature process (600-800$^{\circ}C$) represented by which developed the process and

the other one is high temperature process (900-1000$^{\circ}C$) invented by Chemrec[7, 10]. Chemrec and Noell are two companies developing pressurized, high temperature gasifiers [5].

Low Temperature Black Liquor Gasification is based on indirect heating of a fluid bed with tube bundles comprised of pulsed heater tailpipes [11]. The process involves steam reforming of the black liquor. In this process, the temperature is kept low enough such that the smelt doesn't become molten or even reach the point where it becomes sticky [7]. The liquor is gasified at a temperature of 600-800$^{\circ}C$ under reducing conditions [12]. A schematic of a typical reformer/gasifier system is shown in Figure 4. This system utilizes a fluidized bed of sodium carbonate particles. Steam introduced through the bottom of the vessel serves as the fluidizing gas as well as the source of water for the reforming operation. The black liquor is introduced through a nozzle system also located on the bottom of the vessel. Heat is transferred to the bed through several tube modules that carry hot combustion gas. Heat from the combustion gases is transferred through the walls of the bed tubes to the bed material where the reforming operation occurs [7, 8]. The composition of product gas is mainly hydrogen (≈80%) in addition to carbon dioxide (≈10%) and methane, ethane and propane (≈10%) [11].

In this system, the alkali salts are kept below their melting point. Consequently, no component is exposed to molten salts and most are utilized at temperatures below those encountered in the higher temperature process. The outer surface of the bed tubes will be exposed to a gas mixture that includes hydrogen, hydrogen sulfide, steam, and carbon monoxide and the tubes will also be subjected to the movement of the particles in the fluidized bed. The gases exiting the bed tubes are directed into another chamber that is connected to a heat recovery system. The reformer/gasifier vessel is lined with refractory. The erosive action of the bed particles is a concern in the bed area, while above the bed, degradation of the refractory by the aggressive gases as well as mechanical damage from material condensing on the refractory lining are concerns [8].

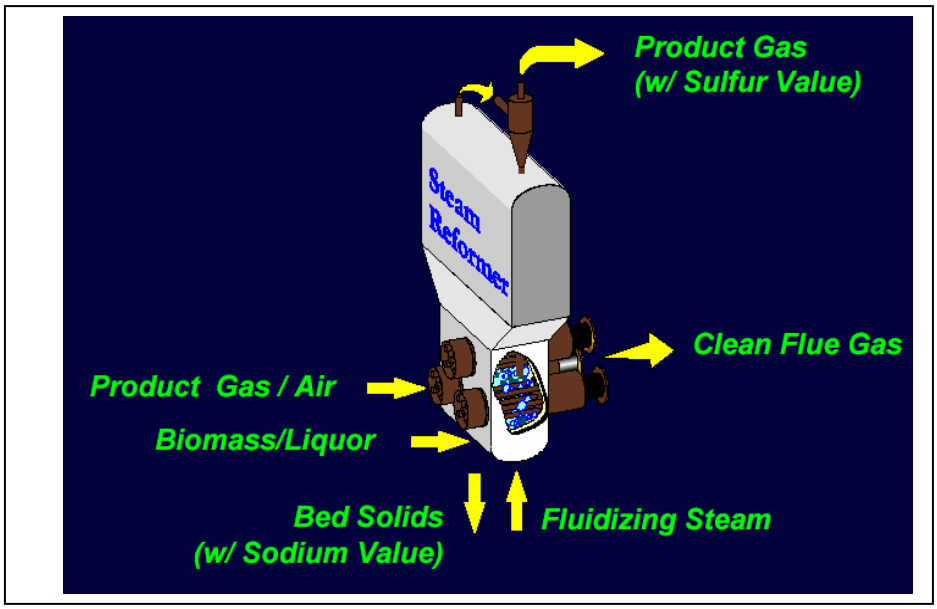

Figure 4 Schematic of steam reformer/gasifier vessel [13]

The high temperature gasification process can be operated near atmospheric pressure or at significantly elevated pressures [7, 8, 14]. A schematic of a high-temperature, low-pressure (HTLP) gasifier is shown in Figure 5. In this refractory lined vessel, the black liquor fuel and the air for partial combustion are injected at the top of the vessel. The organic material contained in the black liquor is gasified and the inorganic salts are left in the liquid state, primarily on the gasifier wall. The liquid and gaseous products are carried out the bottom of the gasifier vessel. The product gas is routed through a gas clean-up system to remove residual particulates and H_2S and the inorganic salts are directed to the green liquor tank [8].

There is some limited experience with high-temperature, high-pressure (HTHP) gasification. A 10 tons/day pilot scale unit has been operated in Sweden. A total of only about 1000 hours operating time was accumulated on black liquor feed [8].

There are two competing designs being considered for the HTHP gasifier. One design utilizes a thick refractory lining within a metal pressure vessel. This design has a refractory lining similar to that shown in Figure 5 for the HTLP. The alternative design, called a cooling screen (Figure 6), utilizes a helically coiled metal tube that has a refractory surface coating and contains pressurized cooling water. Currently, a high-temperature, high-pressure demonstration scale unit is under construction in Sweden. Operation is expected to begin in mid to late 2003 and both the thick refractory lining and the cooling screen design will be tested [8].

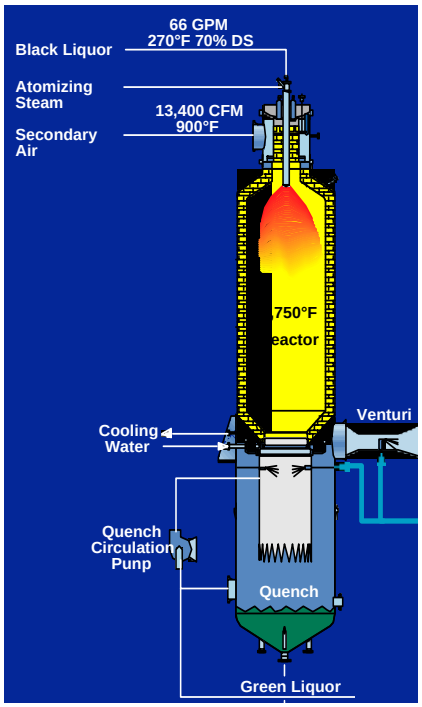

Figure 5 Schematic of high temperature, low pressure gasifier

In the high temperature systems, the units operate at temperatures above the melting point of the inorganic salts, between 900-1000$^{\circ}C$, and at pressures ranging from 2 to 4 MPa, depending on the desired pressure level for gas turbine operation. The synthesis gas is a high value product composed of chemicals such as hydrogen, methanol or ammonia [10].

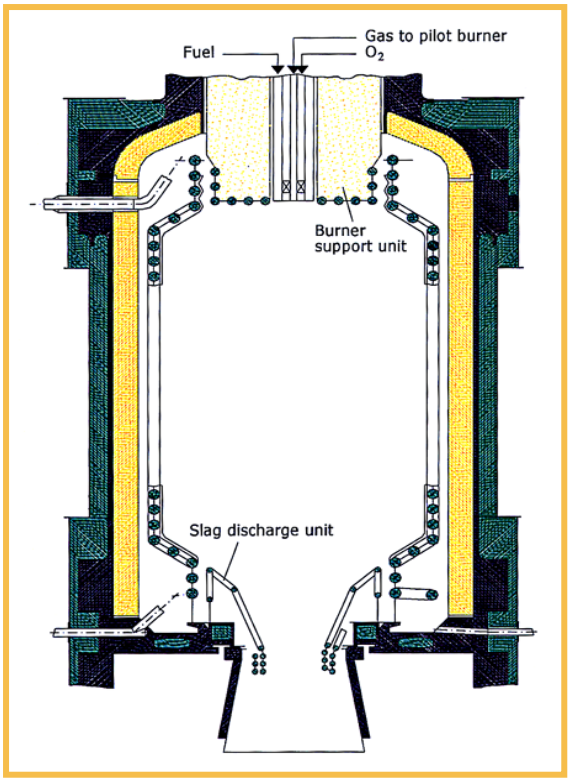

Figure 6 Schematic of high temperature, high pressure gasifier [8]

The core component of the Chemrec system is the gasifier, a refractory lined entrained flow reactor where the black liquor is decomposed under strongly reducing conditions. Preheated air is used as oxidant and reducing atmosphere turns to oxidizing in the starting up or shutting down the furnace. Injection of steam also provides some oxidizing conditions intermittently. The black liquor droplets are dried and partially combusted, producing combustible gas and smelt drops. The dry solids are loaded with alkaline catalyst containing volatiles and a high content of oxygen. Under gasification conditions, black liquor pyrolyses very rapidly. The black liquor is a unique material because of the extremely fine dispersion of sodium (or potassium) throughout the carbon matrix. The high catalyst loading and fine distribution of catalyst is believed to be responsible for the very high gasification rates experienced [3].

It is reported that, during black liquor gasification, sodium and potassium vapors are released in relatively large quantities. Preliminary data indicates that alkali volatilization can be in excess of 20% of the total sodium entering with the black liquor [3]. But equilibrium calculations of black liquor composition at $950^{\circ}C$ under atmospheric pressure, by FactSage database, show that the amount of sodium and potassium vapors in the gasifier atmosphere doesn't exceed 2%. It is also reported that gaseous alkali compounds are formed above $900^{\circ}C$, in the form of diatomic sodium and sodium hydroxide [3]. Furthermore, the total pressure affects the equilibrium amount of alkali in the gas. Higher pressure results in considerably lower alkali release. Lowering the air/fuel ratio results in significantly increased alkali volatilization. In the HTHP process, the reactor pressure increases to 20-40 atm compared to atmospheric pressure which is normally used in HTLP process. As was mentioned, the reactor temperature in the high

temperature process is between 900-1000$^{\circ}C$, normally kept in the 950-975$^{\circ}C$ range [3, 10].

The gaseous atmosphere in the gasifier includes hydrogen, hydrogen sulfide, carbon monoxide, carbon dioxide, nitrogen, methane and steam. In addition, most of the interior surface of the gasifier vessel is exposed to molten salt (Na_2CO_3 and Na_2S) flowing to the outlet of the reactor in a reducing environment. The use of oxygen in place of air provides the possibility of substantially higher gasification temperature, up to 1400$^{\circ}C$ [15].

In Alumino-silicate refractories, the alkali penetrates into the brick structure, reacts with the brick components and results in the formation of expansive phases containing varied combinations of alkali, alumina, and silica. Cracking and spalling occur from the resulting mechanical stresses associated with the formation of these expansive phases. Below approximately 1260$^{\circ}C$, the phases such as nepheline (soda + alumina + silica), leucite and kalsilite (potash + alumina + silica) are formed with a large volume change. Above 1260$^{\circ}C$, the fireclay group typically reacts with the volatile alkali to form a viscous glass. The viscous glassy layer may protect the refractory and stabilize the wear, however, exposure to increased temperature can greatly accelerate the pace of fluxing and wear. Alkali also causes free alumina phases $(\alpha - alumina)$ to recrystallize into $\beta - alumina$ which associates with a large volume expansion. In the experiment accomplished at 1204$^{\circ}C$ for 5 hours on 60% alumina samples mixed with sodium carbonate in different proportions, it was found that the 5% soda pellet appeared relatively unaffected. The 10% soda pellet also appeared relatively unaffected; however, XRD analysis showed the formation of nepheline in some quantity. The 20% sample was weakened and friable, the 30% soda sample showed signs of the initial expansive phase formation followed by the formation of liquid phases and 40% soda sample showed significant shrinkage associated with liquid formation. It means that greater soda levels result in the formation of greater quantities of expansive and/or liquid phases. In the case of 90% alumina mullite bonded samples; soda reacted with both the free alumina and the mullite bond, to form nepheline and $\beta - alumina$. The proposed reactions for the mentioned interaction are as follows [16]:

$$Na_2O + 3Al_2O_3.2SiO_2 \longrightarrow Na_2O.Al_2O_3.2SiO_2 + 2Al_2O_3 \quad (4)$$

$$Na_2O + 3Al_2O_3.2SiO_2 + 2SiO_2 \longrightarrow 3Na_2O.2Al_2O_3.4SiO_2 + Al_2O_3 \quad (5)$$

$$Na_2O + Al_2O_3 \longrightarrow Na_2O.Al_2O_3 \quad (6)$$

$$Na_2O + 11Al_2O_3 \longrightarrow Na_2O.11Al_2O_3 \quad (7)$$

$$Na_2O + SiO_2 \longrightarrow Na - Si(Glass) \quad (8)$$

Yamaguchi, A. has reported that the exposure of $\beta - alumina$ powder to K_2CO_3 vapor at 1200$^{\circ}C$ changes the composition from $Na_2O.11Al_2O_3$ to $0.977K_2O.0.023Na_2O).7.5Al_2O_3$ as a result of substitution of K for Na. The lattice constant of c of $\beta - alumina$ changed from 22.54$^{\circ}A$ to 22.73$^{\circ}A$ in addition to formation of a great number of cleavages vertical to the c axis of the crystal [17]. More over it is reported that when fireclay refractories composed of mullite and silica is exposed to Na_2CO_3 vapor, the main product is nepheline (NAS_2), but in the case of high

alumina refractories composed of corundum and mullite the main reaction product is carnegieite s.s $(NAS_2 - NAs.s)^*$. Interaction of corundum with K_2CO_3 vapor, results in the formation of potassium aluminate and interaction of mullite with K_2CO_3, results in the formation of $KAS - KAs.s^*$ [2]. When $Al_2O_3 - ZrO_2 - SiO_2$ system refractories composed of corundum, baddeleyite and a glassy phase approaching the composition of albite $(NAS_6)^*$, is exposed to sodium carbonate, nepheline and carnegieite s.s $(NAS_2 - NAs.s)^*$ are formed as a result of interaction of alumina and albite with sodium carbonate and sodium zirconate is formed as a result of interaction of baddeleyite with sodium carbonate. In the case of exposure to K_2CO_3 vapor, $(K, Na)AS_2^*$ (kalsilite) and $KAS - KAs.s^*$ are formed as the result of interaction of alumina and albite with $\mathrm{K_2CO_3}$ vapor and K_2O-rich glass is formed as a result of interaction of baddeleyite with K_2CO_3 vapor [17].

Silica refractories exposed to sodium and potassium carbonate vapor at $1370^\circ C$ shows excessive corrosion and depth of reaction. The reaction of potash appears to be more aggressive. Cracking and spalling were observed in mullite bricks in potash environment as a result of formation of potassium aluminate and potassium aluminum silicate. The porosity of the sample has a considerable effect on the degree of corrosion. A high degree of inter-joint reaction with silica especially in the potash test was observed. Bonded AZS^* composition shows substantial improvement over zircon with respect to degree of reaction with alkali vapors but is still vulnerable to spalling. A decrease in alumina content and lower apparent porosity tend to improve resistance to potash vapor. Fused alumina shows negligible interface reaction but tends to demonstrate a high degree of inter-joint reaction with silica [18].

N. R. Brown has reported that Na_2O reacts rapidly with high silica refractories, %10 Na_2O will form 50% liquid at temperatures as low as $1100^\circ C$. In the case of mullite refractories, formation of expansive phases such as $NaAlO_2$, $\beta - Al_2O_3$ and carnegieite at low temperatures, and formation of liquid phases at $T \geq 1000^\circ C$ is proposed to be the failure mechanism [4]. In the case of exposure to K_2O, high silica refractories form leucite $(KAS_4)^*$. Kaliophilite $(KAS_2)^*$ appears in the fireclay refractories and at about 60% Al_2O_3, $K - \beta - Al_2O_3$ is formed. In the case of high alumina refractories $K_2O.Al_2O_3$ (potassium aluminate) is formed as well as $K - \beta - Al_2O_3$ [19].

C. R. Kennedy who studied alkali attack on mullite refractories in coal gasifier, detected $NaOH$ in the samples in the case of existence of water vapor. The proposed corrosion reaction he proposed is as follows:

$$11(Al_6Si_2O_{13}) + 26(NaOH) \longrightarrow 22(NaAlSiO_4) + 4(NaAl_{11}O_{17} + 13H_2O) \quad (9)$$

In $\mathrm{Na_2O\text{-}SiO_2\text{-}Al_2O_3}$ phase diagram and according to the lever rule, a reaction between a Na compound and mullite should produce $\sim$ 40wt% $\beta - \mathrm{Al_2O_3}$ and $\sim$ %60 nepheline with $\sim$ %30 volume expansion which easily explains the failure cause. It is also reported that at 900-$1400^\circ C$, the corrosion by alkali compounds slows down by the increase in the alumina content of aluminous refractories. Formation of

β - alumina was observed only at temperatures in excess of $1100^{\circ}C$. At $950^{\circ}C$, high silica (~%60) refractories performed better because of the ability of high silica refractories to react more rapidly with the alkali and contain its attack at the surface [20]. Sodium sulfate condensation as a result of reaction between sodium vapor and sulfur oxides and formation of nepheline $(754 - 954^{\circ}C)$ and noselite $(1150^{\circ}C)$ is reported to be the cause of bloating in fireclay refractories. Noselite is a nepheline sulfate mineral: $6(NaAlSiO_4).Na_2SO_4$, resulting from the conversion of nepheline by sodium sulfate. Reducing conditions enhances the formation nepheline [21].

Barrie H. Bieler found that among Na_2CO_3, Na_2SO_4 and $NaCl$, the most corrosive material on Alumina-Zirconia-Silica refractories is Na_2CO_3 and the least with $NaCl$. He suspended AZS refractories over molten Na_2CO_3 at $1371^{\circ}C$. He tested other types of refractories over different types of salts as well. If water vapor present, formation of $NaOH$ is probable because of interaction of sodium carbonate and water. It is reported that at higher temperatures up to $1470^{\circ}C$, the chemical species are not only liquid Na_2CO_3 but also some liquid $NaOH$ and gaseous CO_2, H_2O and Na_2O. The major crystalline species in AZS refractories is monoclinic ZrO_2; the minor one is alpha alumina. SiO_2 is present only as an aluminosilicate glass. In the samples exposed to alkali vapors, different zones appeared. The gray central core grades into a more bleached zone, which is more pronounced in the case of exposure to Na_2CO_3 vapor. This then grades into a zone one millimeter wide which is slightly yellow composed of smaller crystals of monoclinic ZrO_2 with a wicker pattern of $\alpha - Al_2O_3$. In this yellow band, the original dendritic texture of ZrO_2 is broken up into smaller aggregates of ZrO_2 crystalline masses. The outermost layer, mottled white and light gray, is locally very porous and has a "warty" outer surface. This zone appears to be composed of porous aggregates of poorly crystalline material composed of mixed hydrated carbonates and hydroxides of sodium in both the $NaOH$ and Na_2CO_3 vapor corroded samples. Sodium aluminate, $NaAlO_2$ may be present in minor amounts [22].

R. A. Peascoe et al, reported the behavior of mullite, $MgAl_2O_4$ spinel, MgO, alumina, alumina-chromia based and Si_3N_4 refractories exposed to black liquor at $1000^{\circ}C$. In the case of mullite based refractories, molten smelt attacks mullite and forms sodium aluminum silicates accompanied by a dramatic volume change. $MgAl_2O_4$ refractories in in the case of polycrystalline spinel in MgO matrix showed minimal penetration and reaction due to minimal porosity or lack of α-alumina in the matrix. Fused spinel containing large spinel crystals was altered from the surface due to low porosity and slow diffusion of smelt. Samples containing $\alpha - alu\,\min a$ or components such as $CaAl_4O_7$ in the matrix are not resistant. Minimal reaction was observed in MgO based refractories but $\beta - Si_3N_4$ sample dissolved in the molten smelt. Molten smelt were found in the interior of the chromia/alumina sample with the primary reaction products of sodium aluminate and chromate [23].

Tadaoki Fukui et al reported that the reactivity of each sodium compound would be in the following descending order [24]:

$$Na_2CO_3 > Na_2SO_4 > NaCl \qquad (10)$$

This can be expected from the dissociation constants of these compounds:

$$K_{Na_2CO_3} = 1 \times 10^{-3} \qquad \text{at } 1400^\circ C \qquad (11)$$

$$K_{Na_2SO_4} = 1 \times 10^{-9} \qquad \text{at } 1400^\circ C \qquad (12)$$

$$K_{NaCl} = 1 \times 10^{-13} \qquad \text{at } 1450^\circ C \qquad (13)$$

They reported that a high reactivity vapor, sodium carbonate, is caught at the surface of refractory but the lower reactivity vapors, sodium sulfate and sodium chloride, infiltrated into the specimens through the pores and interstices around the grains [24].

EXECUTIVE SUMMARY

Black liquor gasification is a high potential technology for production of energy which allows substitution for other sources of energy. This process uses a waste of the pulp and paper industry as black liquor to produce synthetic gas and steam for production of electricity; therefore development of this technology not only recovers the waste of the paper industry but also decreases dependency on fossil fuel.

Today one of the main obstacles in the development of this technology is the development of refractory materials for protective lining of the gasifier. So far the materials used for this application have been based on alumino-silicate refractories but, thermodynamics and experience shows that these materials are not sufficiently resistant to black liquor under the harsh working condition of Black liquor gasifiers. Consequently development of cost-effective materials with improved performance in gasifier environments to answer the material challenges presented by black liquor gasification (HTHP, HTLP) is the objective of this project.

FactSage thermodynamic modeling software can convert the elemental analysis composition of the black liquor to compound composition. This results show that at 950ºC, black liquor smelt flowing on the refractory lining installed on the gasifier vessel shell is composed of 70-75% sodium carbonate, 20-25% sodium sulfide and 2-5% potassium carbonate. Sodium and potassium carbonate are molten at 950ºC while sodium sulfide is in solid state if it is assumed that there is no solution between sodium sulfide and carbonates. Obviously, the selection of refractory materials for this application should be based upon resistance to molten Na_2CO_3 although Na_2S and K_2CO_3 should not be ignored.

Thermodynamic data shows that none of refractory compounds in the alumino-silicate system are resistant to black liquor. At 950ºC , corundum converts to β"-alumina, β-alumina and K-β-alumina while mullite converts to nepheline, albite, leucite and corundum in contact with Black Liquor. All these phase transformations are associated with large volume expansion. Also thermodynamic data shows that simple oxides including ZrO_2, CeO_2, La_2O_3, Y_2O_3, Li_2O, MgO and CaO are resistant to black liquor but non-oxides such as SiC and Si_3N_4 are oxidized and dissolved in black liquor. Ellingham diagram presents us with the fact that all candidate refractory simple oxides are resistant to both sodium and potassium metal vapors at operating temperature of BLG and none of them are reduced to metallic form.

The other candidates for BLG application are aluminates including $MgAl_2O_4$, $BaAl_2O_4$ and $LiAlO_2$. FactSage database show that none of the aluminates are resistant to sodium oxide in the range of operating temperature of high temperature black liquor gasifier although all three are resistant to sodium carbonate. They form $NaAlO_2$ in contact with sodium oxide. It was observed that none of the aluminates are resistant to potassium oxide and potassium carbonate except lithium aluminate which is stable with potassium carbonate. The reaction product of aluminates with potassium oxide or carbonate is $KAlO_2$.

EXPERIMENTAL

FactSage 5.1 is a thermodynamic database which can be used to do thermodynamic equilibrium calculation. This database can used to find the main refractory compounds formed in the aluminosilicate system or Al-Si-O system. This data base shows that the main refractory compounds in Al-Si-O system are alumina, aluminum silicate (andalusite, silimanite and kyanite) and mullite as follows:

Al_2O_3	FACT S1 S2 S3 S4 L
Al_2SiO_5	FACT S1 S2 S3
$Al_6Si_2O_{13}$	FACT S

As sodium carbonate is the main corrosive component of black liquor smelt in contact with refractories, the interaction of refractory components in Al-Si-O system with sodium components is important. Therefore, FactSage software was used to predict the refractory behavior in contact with Na_2CO_3 at $950^\circ C$ and P_t=1atm, based on Gibbs Free Energy minimization. Phase diagrams shown in the appendix were created using FactSage for the systems of interest.

ABAQUS is a suite of engineering simulation programs, based on the finite element method. ABAQUS can be used to model simple linear systems to complex nonlinear simulations. It contains a library of elements that can be used to model almost any geometry and a list of material models to simulate the behavior of most typical engineering materials. Additionally, for non-typical materials (refractories) material models can be developed using standard FORTRAN programs. It can be used to solve static, dynamic, thermal and non-linear response. Therefore, ABAQUS is being used to model the failure of refractory systems due to expansive reactions. Additionally, when the behavior of the materials is adequately modeled this model will be expanded to the containment system.

RESULTS AND DISCUSSION

The gas phase reaction products are mainly CO_2 with a minor amount of CO and very small amount of sodium and sodium oxide vapor. Solid and liquid phase products are listed in Table 1.

Table 1 Interaction of alumino-silicate refractory compounds with sodium carbonate at 950ºC.

Refractory Compound / Reaction Product	Corundum	Aluminum Silicate	Mullite
Corundum	-	×	×
β-Alumina	×	-	-
Nepheline	-	×	×
Albite	-	×	×

(×): the phase is formed, (-): the phase is not formed

Black liquor is the material used in gasifiers as a raw material to produce energy. Therefore the composition of black liquor is of high importance, because of its huge effect on corrosion behavior of refractory material as a lining of gasifier vessel. The typical composition of virgin black liquor from North American wood is mentioned in Table 2.

Table 2 Typical composition of virgin black liquor from North American wood (wt. %) [25]

	Softwood		Hardwood	
	Typical	Range	Typical	Range
Carbon, %	35.0	32-37.5	34.0	31-36.5
Hydrogen, %	3.5	3.4-4.3	3.4	2.9-3.8
Nitrogen, %	0.1	0.06-0.12	0.2	0.14-0.2
Oxygen, %	35.4	32-38	35.0	33-39
Sodium, %	19.4	17.3-22.4	20.0	18-23
Potassium, %	1.6	0.3-3.7	2.0	1-4.7
Sulfur, %	4.2	2.9-5.2	4.3	3.2-5.2
Chlorine, %	0.6	0.1-3.3	0.6	0.1-3.3
Inert, %	0.2	0.1-2.0	0.5	0.1-2.0
Total, %	100.0		100.0	

The composition of black liquor listed in Table 2 is in the form of elemental analysis but by the use of FactSage as a tool of thermodynamic modeling one can convert elemental analysis compositions to compound compositions as is observed in Table 3 which represents a typical composition of black liquor at $950^{\circ}C$ and P_t=1atm fed to the gasifier.

Table 3 Composition of Black Liquor (wt. %)

Constituents	Na_2CO_3	Na_2S	K_2CO_3	C
%	50-55	25-30	1-3	15-20

If it is assumed that all the carbon is burned by the air introduced to the gasifier, the composition of the smelt in contact of refractory lining will be approximately the composition shown in Table 4.

Table 4 Composition of Black Liquor and melting point of each component (wt. %)

Constituent	**Na_2CO_3**	**Na_2S**	K_2CO_3
%	**70-75**	**20-25**	2-5
Melting Point (^{0}C)	858	1172	901

Therefore, it is observed that about three quarters of the black liquor smelt is composed of sodium carbonate which is liquid in the operating conditions of black liquor gasifiers. Obviously the selection of refractory materials for this application should be based upon resistance to molten sodium carbonate although Na_2S and K_2CO_3 should not be ignored. The melting temperatures of the main components of black liquor are listed in Table 4. It is obvious that Na_2S is not as corrosive as two other components from the point of chemical attack because it is in solid state at the operating conditions of the BLG gasifier while sodium and potassium carbonate are in the liquid state. Obviously this statement is true only when there is no solution between Na_2CO_3 and Na_2S which based on FactSage, no solution was observed.

If refractory compounds in Al-Si-O system, are in contact with Black Liquor at $950^\circ C$ and P_t=1atm, the reaction products based on FactSage data base Gibbs free energy minimization are tabulated in Table 5. The gas phase reaction products include mostly CO and H_2 with minor amounts of H_2O, CO_2, CH_4, NaCl, KCl, N_2, $(NaCl)_2$, H_2S, Na, $(KCl)_2$ and K.

Table 5 Interaction of alumino-silicate compound refractories with black liquor at $950^\circ C$

Refractory Compound / Reaction Product	Corundum	Aluminum Silicate	Mullite
Corundum	-	×	×
β"-alumina	×	-	-
β-alumina	×	-	-
k-β"-alumina	×	-	-
Nepheline	-	×	×
Albite	-	×	×
Leucite	-	×	×
Na_2S	×	-	-
Graphite	×	×	×

(×): the phase is formed, (-): the phase is not formed

It is obvious from the information in Tables 2 and 5 that none of the alumino-silicate refractories, even α-alumina, are resistant to either sodium carbonate or Black Liquor at $950^\circ C$ which is the temperature of gasification in both HTHP and HTLP processes. It is observed that all α-alumina is converted to $\beta-$alumina in contact with Na_2CO_3 and to

β"-alumina, $\beta-$alumina and $K-\beta-$alumina in contact with Black Liquor. All formed phases are in the solid state in black liquor gasification conditions. Therefore, large volume changes due to formed phases should impose large stresses in refractory structure. In this condition it is predicted that crack formation and spallation of refractory may be the main wear mechanism.

In the case of mullite; nepheline, albite, leucite and corundum are formed just based on thermodynamic equilibrium calculations. All of these phases are in the solid state and have large volume changes which are enough to produce large cracks in the structure and decrease the lining life considerably due to spallation. In this case, α-alumina formed as a reaction product of mullite with black liquor can be attacked again with black liquor and corroded by the same mechanism.

The same occurs for aluminum silicate compounds with some differences in the amount of new phases formed as a result of interaction of these compounds with Black Liquor at $950^{\circ}C$. The vaporization of refractory constituents is negligible in these conditions.

Historically the refractory materials used as the lining of high temperature black liquor gasifiers to protect the vessel have been based on alumino-silicates refractories which predictably cannot survive for a long time. The interaction between these refractories and sodium carbonate is proposed to be as follows:

$$Na_2CO_3 + SiO_2 \longrightarrow Na_2O.SiO_2(glass) + CO_2 \quad (1)$$

$$Na_2CO_3 + Al_2O_3 \longrightarrow Na_2O.Al_2O_3 + CO_2 \quad (2)$$

$$Na_2CO_3 + 11Al_2O_3 \longrightarrow Na_2O.11Al_2O_3(\beta - Alu\min a) + CO_2 \quad (3)$$

$$Na_2CO_3 + 3Al_2O_3.2SiO_2 \longrightarrow Na_2O.Al_2O_3.2SiO_2 + 2Al_2O_3 + CO_2 \quad (4)$$

$$Na_2CO_3 + 3Al_2O_3.2SiO_2 + 2SiO_2 \longrightarrow 3Na_2O.2Al_2O_3.4SiO_2 + Al_2O_3 + CO_2 \quad (5)$$

The information obtained from use of the FactSage thermodynamic data base regarding alumino-silicate refractories in contact with Black Liquor only relates to thermodynamics if equilibrium is achieved and the kinetics are not considered. Experimental verification is necessary to discover the corrosion mechanism.

Some thermodynamic studies (FactSage) were performed to predict the behavior of some simple refractory oxides and complex oxides, as well as non-oxides as new refractory material candidates, against Na_2O, Na_2CO_3, K_2O, K_2CO_3, the main components of black liquor.

Simple oxides selected as candidates for use in high temperature black liquor gasifier are Al_2O_3, SiO_2, ZrO_2, CeO_2, La_2O_3, Y_2O_3, MgO and CaO. In first step an effort was made to plot an Ellingham Diagram for these oxides against sodium oxide (and also potassium oxide) to see the potential of sodium or potassium metal vapor to reduce the candidate refractory oxides because the existence of alkaline metal vapor in the gasifier atmosphere is probable. Obviously if the free energy of formation of each candidate is less than that for sodium or potassium oxide, it means that that oxide is more stable than sodium (potassium) oxide or sodium (potassium) metal vapor is not able to reduce it. Therefore that oxide is stable and can be still be a candidate for use in our application conditions. It should be mentioned that the total pressure (P_t) selected to plot the diagram is 1 atmosphere. The plotted diagram is presented in Figure 7.

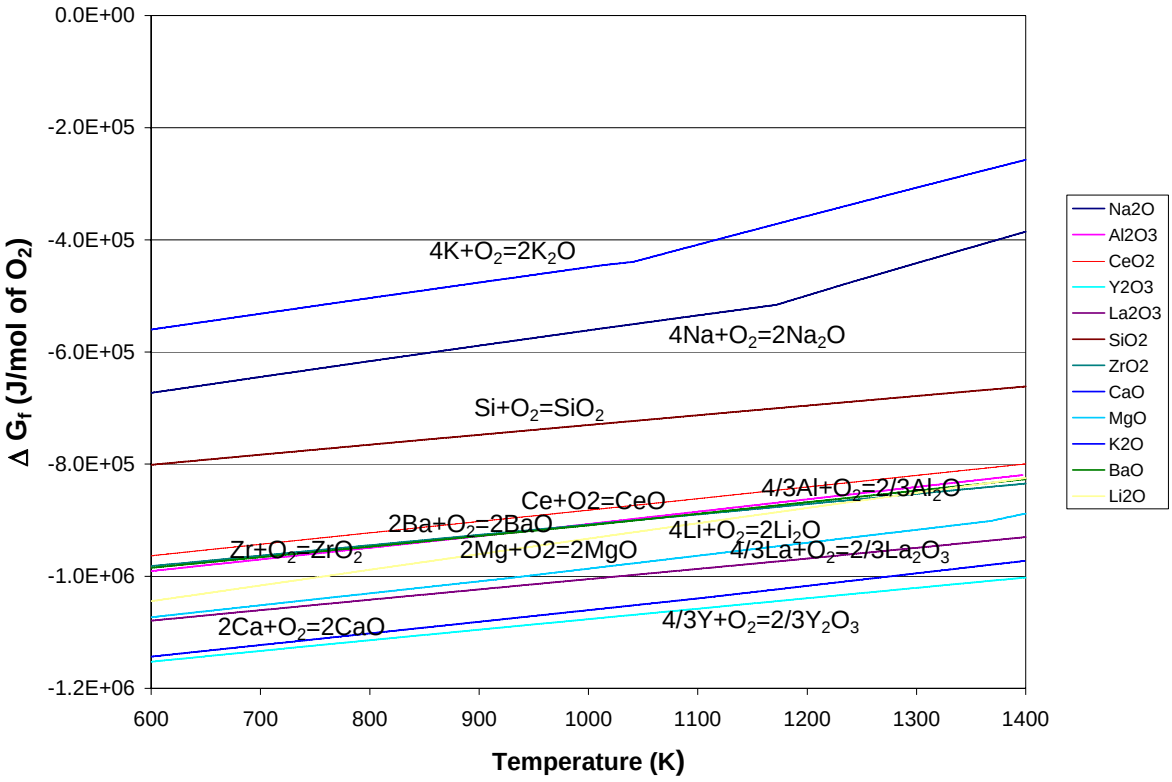

Figure 7 Ellingham Diagram of candidate simple oxides against sodium oxide

As is seen from the diagram, all of candidate refractory simple oxides are resistant to sodium metal vapor or potassium as well at P_t=1atm and T = 600 - 1400K because they all have free Gibbs Energy of formation, less than that of sodium or potassium oxide. But also it should be mentioned that Ellingham Diagram can not be the only tool to evaluate the material because it doesn't show any data in the case that new compounds are formed. For example, alumina or silica is not reduced by sodium oxide but they form new compounds which are the cause of wear.

FactSage was also used to predict the behavior of candidate refractory simple oxides against the main components of black liquor at T=900-1000$^\circ C$ which is the working temperature range of high temperature BLG gasifier. The results are listed in Table 6. It shows that all our simple oxide refractories except Al_2O_3 and SiO_2 are resistant against sodium and potassium oxide and sodium and potassium carbonate.

More over, it is observed that based on the FactSage thermodynamic data base, SiC and Si_3N_4, two non-oxide refractory candidates for BLG gasifier applications, are not resistant to black liquor constituents. SiC is converted to compounds such as $(Na_2O)(SiO_2)$, $Na_6Si_2O_7$, K_2SiO_3 and $K_2Si_2O_5$ which some of them are in liquid state in operating temperature on BLG gasifier and dissolved into the smelt.

Table 6 Interaction of refractory simple oxides and non-oxide with BLG components at T=900-1000ºC

Refractory	Na_2O	Na_2CO_3	K_2O	**K_2CO_3**
Al_2O_3	×	×	×	×
SiO_2	×	×	×	×
MgO	-	-	-	-
CaO	-	-	-	-
ZrO_2	-	-	-	-
Y_2O_3	-	-	-	-
La_2O_3	-	-	-	-
CeO_2	-	-	-	-
Li_2O	-	-	-	-
BaO	×	×	×	×
SiC	×	×	×	×
Si_3N_4	×	×	×	×

(×): reaction, (-): no reaction

There is some concern regarding the hydration of two of the oxides, MgO and CaO especially when the operating condition of the gasifier includes water vapor. Therefore an effort was made to predict the hydration behavior of these oxides as a function of temperature at P_{H_2O} = 1, 20 and 100atm. The FactSage data base was used and the results of this study are listed in figures 8 and 9.

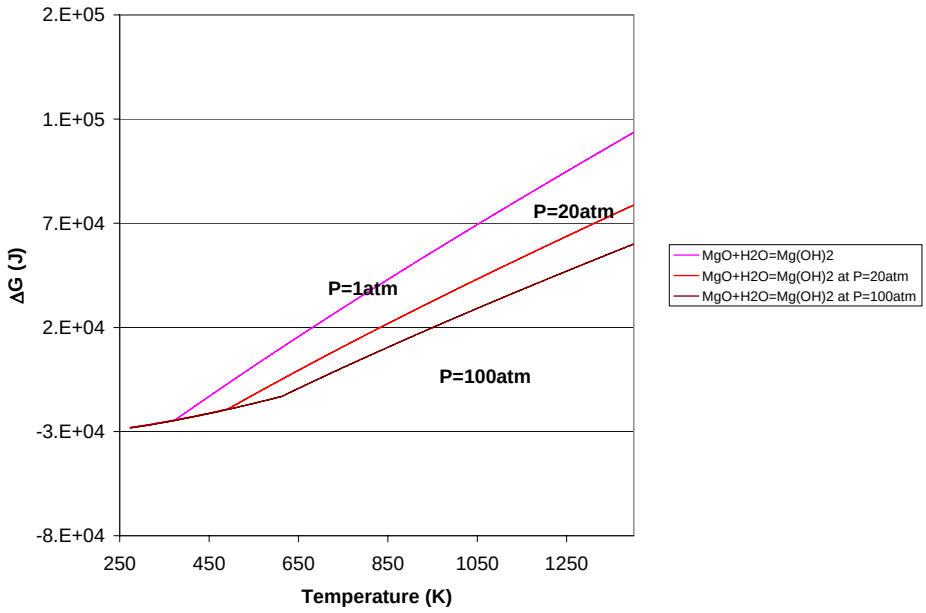

Figure 8 Hydration behavior of Magnesia

There is a temperature gradient across the refractory lining, the hydration depends on penetration of water vapor into the depth of refractory lining through porosity, cracks or joints. As it is observed from Figure 8 even at P_{H_2O} = 100atm, hydration doesn't occur for

magnesia until temperatures less than $500^{\circ}C$ but under the same conditions, calcia hydrates easily at about T=$950^{\circ}C$. Therefore, it can be concluded that perhaps magnesia can be used in BLG gasifiers but calcia would have the problem of hydration because diffusion of water vapor into the refractory lining to reach the limiting hydration temperature is much more probable for calcia compared to magnesia.

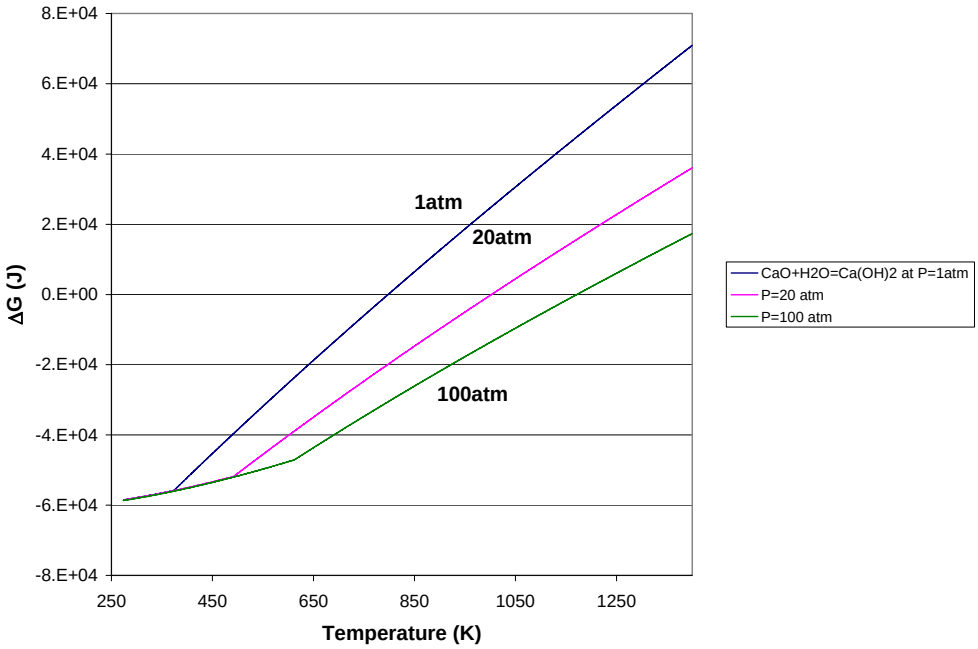

Figure 9 Hydration behavior of Calcia

The next step is to study the behavior of aluminates with alkaline atmospheres. The candidate aluminates are $MgAl_2O_4$, $BaAl_2O_4$, $LiAlO_2$ and the equation for the main corrosion reaction of these oxides with sodium oxide are as follows:

$$MgAl_2O_4 + Na_2O \longrightarrow MgO + 2NaAlO_2 \qquad (6)$$

$$BaAl_2O_4 + Na_2O \longrightarrow BaO + 2NaAlO_2 \qquad (7)$$

$$2LiAlO_2 + Na_2O \longrightarrow Li_2O + 2NaAlO_2 \qquad (8)$$

The change in the free Gibbs Energy (ΔG) because of reaction is plotted versus temperature in Figure 10. The data to plot this diagram was provided from the FactSage data base.

From this diagram it is understood that none of the aluminates are resistant to sodium oxide in the range of temperature 600-1400K because ΔG for reaction for all of them with sodium oxide is negative although it can be concluded that barium aluminate is the most resistant one and magnesium aluminate is the least resistant one against sodium oxide.

As sodium is in the form of sodium carbonate and not sodium oxide in black liquor and in the working conditions of high temperature gasifiers therefore it is worth while to try to predict the behavior of these aluminates to sodium carbonate as well.

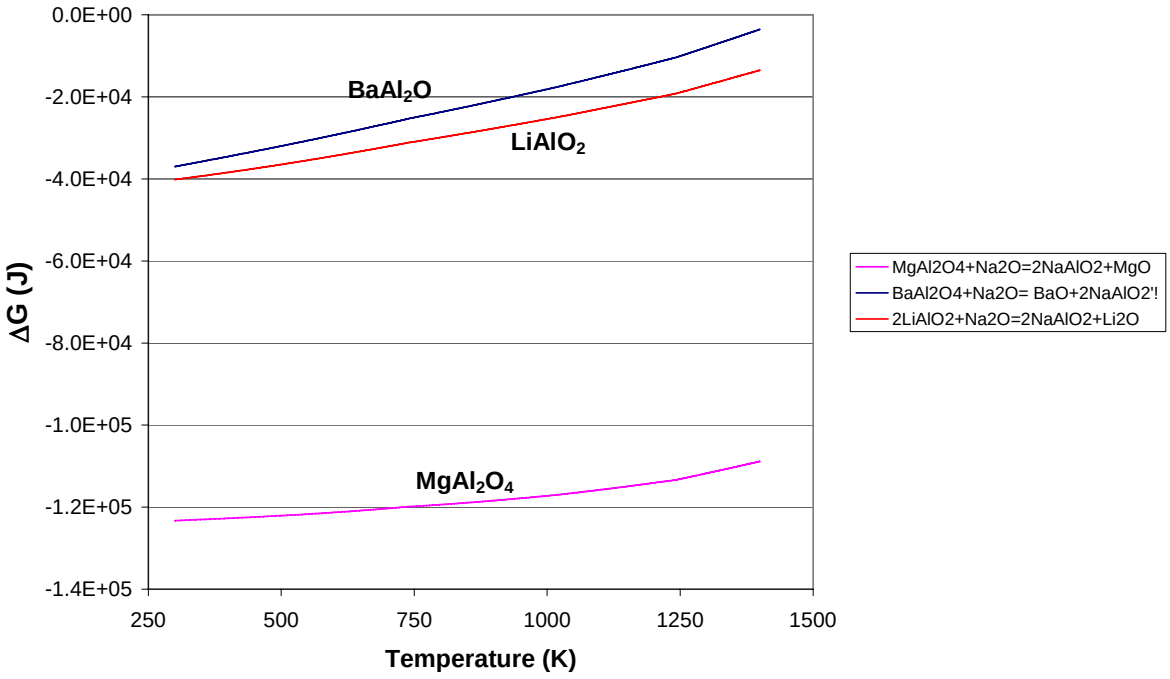

Figure 10 ΔG for the reaction between three candidate aluminates with sodium oxide

The reaction equations of candidate aluminates with sodium carbonate are as follows:

$$MgAl_2O_4 + Na_2CO_3 \longrightarrow MgCO_3 + 2NaAlO_2 \qquad (9)$$

$$BaAl_2O_4 + Na_2CO_3 \longrightarrow BaCO_3 + 2NaAlO_2 \qquad (10)$$

$$2LiAlO_2 + Na_2CO_3 \longrightarrow Li_2CO_3 + 2NaAlO_2 \qquad (11)$$

First we should know the ranges of temperatures over the carbonate products are stable. The reaction equations for stability of the three above listed reactions (the diagram for K_2CO_3 and $CaCO_3$ is plotted as well) are as follows:

$$MgCO_3 \longrightarrow MgO + CO_2 \qquad (12)$$

$$BaCO_3 \longrightarrow BaO + CO_2 \qquad (13)$$

$$Li_2CO_3 \longrightarrow Li_2O + CO_2 \qquad (14)$$

$$Na_2CO_3 \longrightarrow Na_2O + CO_2 \qquad (15)$$

ΔG for dissociation of carbonates as a function of temperature in the range of 600-1400K based on FactSage thermodynamic data base is shown in Figure 11.

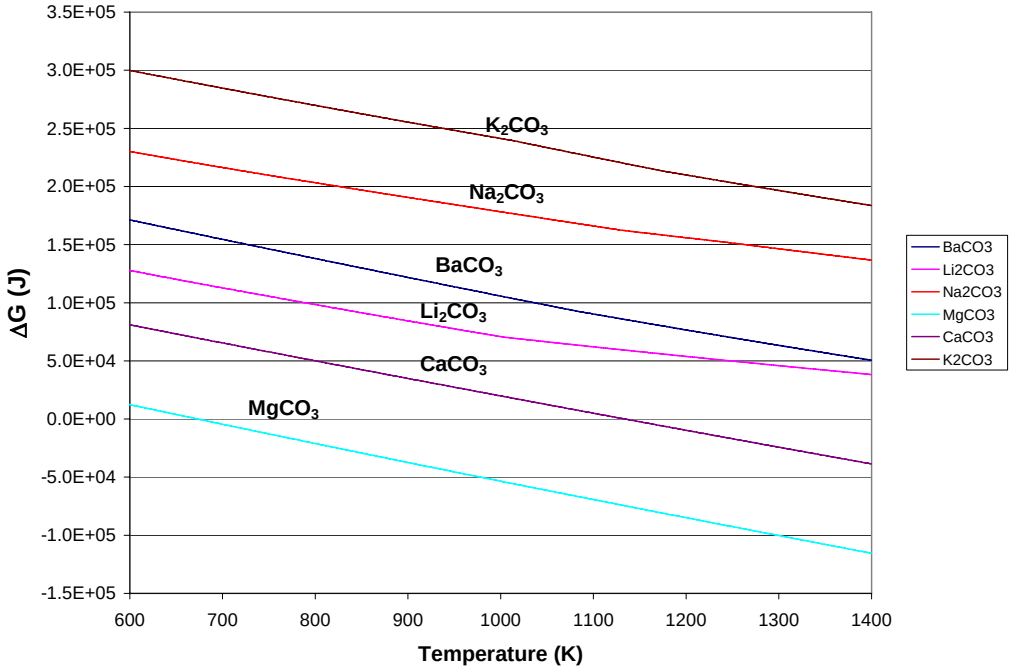

Figure 11 ΔG of dissociation of carbonates versus temperature

From Figure 11 it is recognized that all considered carbonates as reaction products of aluminates with sodium carbonate are stable except magnesium carbonate which dissociates at 673K and P_t = 1atm. The same happens to calcium carbonate but at higher temperature. Therefore from T=637K, the equation for the reaction of magnesium aluminate with sodium carbonate should change to the reaction as follows:

$$MgAl_2O_4 + Na_2CO_3 \longrightarrow 2NaAlO_2 + MgO + CO_2 \qquad (16)$$

Also it can be seen that sodium and potassium oxide are not in the form of an oxide in the range of working temperatures of BLG gasifiers but they are in carbonate form.
Now following the reactions mentioned above, thermodynamic stability of aluminates against sodium carbonate can be evaluated based on FactSage data base. Figure 12 is the result of this thermodynamic modeling in the form of ΔG of reaction versus temperature. It is observed that all candidate aluminates are stable against sodium carbonate and among them magnesium aluminate spinel is the most resistant because it has the highest change of Free Gibbs Energy as a result of reaction with sodium carbonate.
It is hard to decide whether to candidate these aluminates for the lining of high temperature gasifiers because, although they are resistant to sodium carbonate, they are corroded by sodium oxide. Thermodynamic modeling shows that sodium is stable in the form of sodium carbonate and sodium sulfide in the operating conditions of high temperature black liquor gasifier and not in the form of sodium oxide, but it seems to be risky to use these refractory materials in these conditions because existence of sodium oxide due to introduction of water vapor to the gasifier and unstable operating condition is probable.

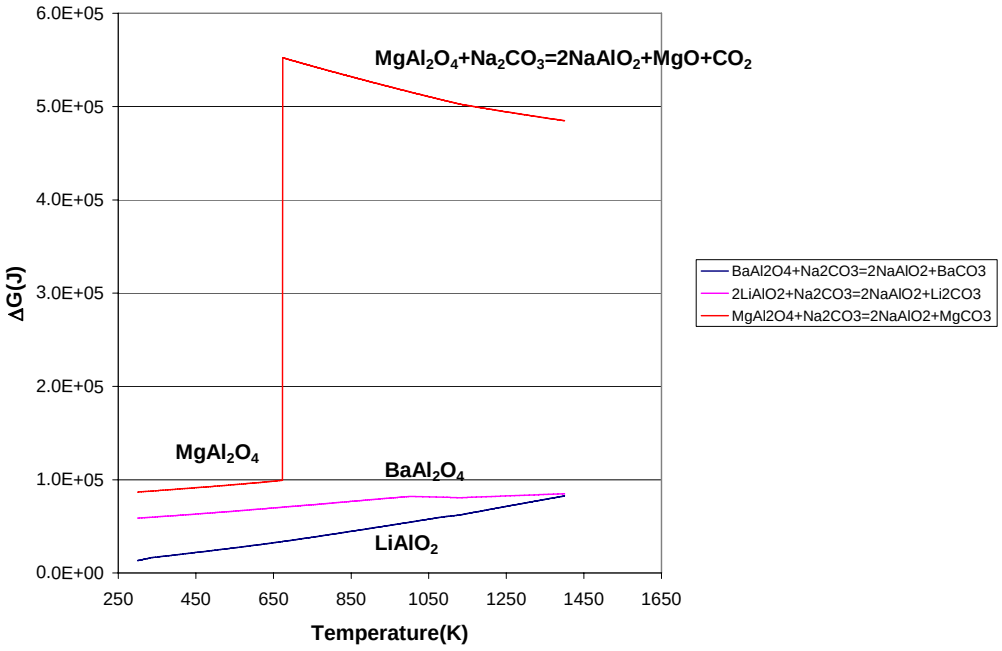

Figure 12 ΔG of reactions between aluminates and sodium carbonate

Thermodynamic modeling of reaction of aluminates with black liquor composition shows that they are not resistant to potassium containing compounds of black liquor; therefore, it was decided to study the reaction behavior of aluminates with K_2O and K_2CO_3 as well. The main reaction of three aluminates with potassium oxide is as follows:

$$MgAl_2O_4 + K_2O \longrightarrow MgO + 2KAlO_2 \quad (17)$$

$$BaAl_2O_4 + K_2O \longrightarrow BaO + 2KAlO_2 \quad (18)$$

$$2LiAlO_2 + K_2O \longrightarrow Li_2O + 2KAlO_2 \quad (19)$$

Free Gibbs energy change of the reaction as a function of temperature is plotted in Figure 13.

It is observed that none of our candidate aluminates resist potassium oxide and, among them, barium aluminate is the most resistant one and magnesium aluminate is the least. Reaction equations of aluminates with potassium carbonate are as follows:

$$MgAl_2O_4 + K_2CO_3 \longrightarrow MgCO_3 + 2KAlO_2 \quad (20)$$

$$BaAl_2O_4 + K_2CO_3 \longrightarrow BaCO_3 + 2KAlO_2 \quad (21)$$

$$2LiAlO_2 + K_2CO_3 \longrightarrow Li_2CO_3 + 2KAlO_2 \quad (22)$$

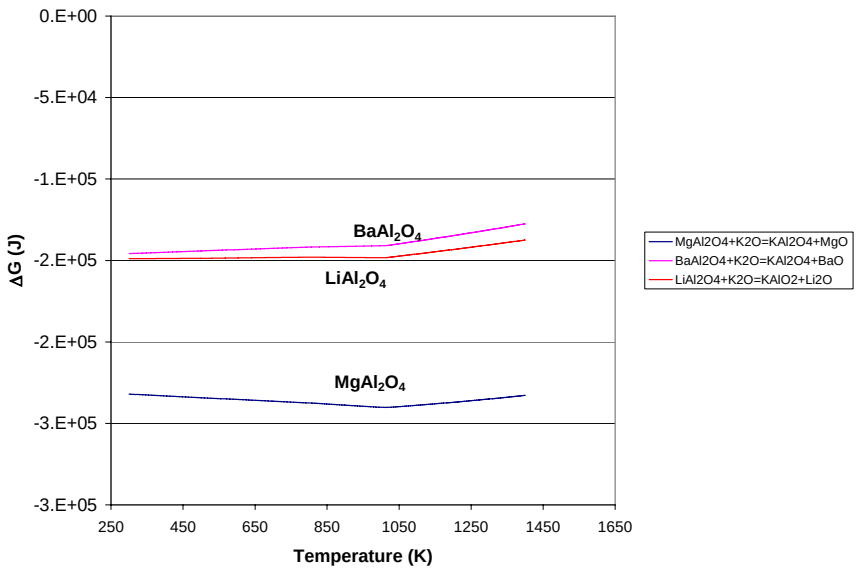

Figure 13 ΔG of reactions between aluminates and potassium oxide

ΔG of reactions between aluminates and potassium carbonate versus temperature are plotted in Figure 14. It can be concluded from this figure that among the three aluminates, only lithium aluminate is resistant to potassium carbonate and the usage of barium and magnesium aluminates in exposure to potassium carbonate is not advisable. It can be summarized that all three aluminates are resistant to sodium carbonate, but not sodium oxide. Also it was observed that none of the aluminates are resistant to potassium oxide, but, regarding potassium carbonate, lithium aluminate is resistant.

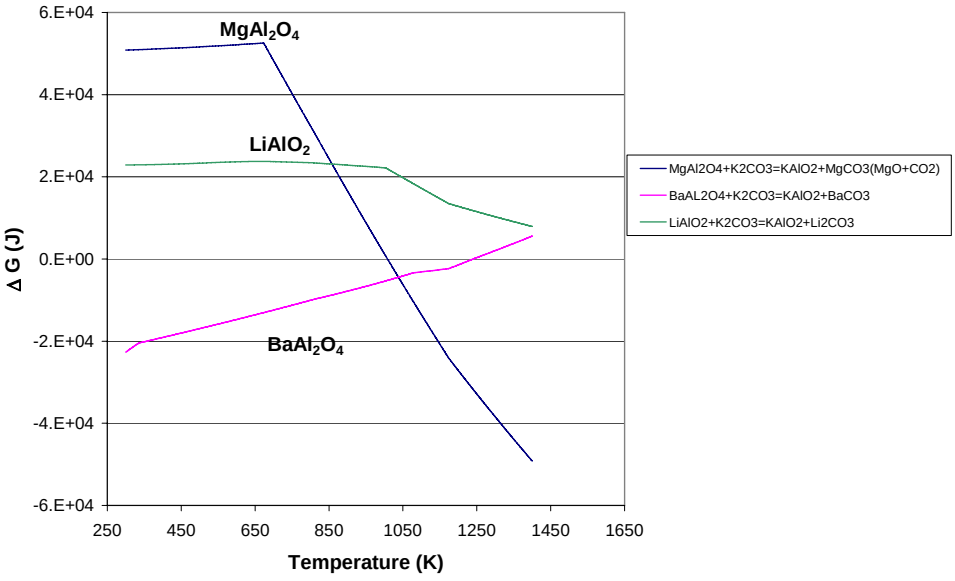

Figure 14 ΔG of reactions between aluminates and potassium carbonate

CONCLUSION

Worldwide growth of black liquor production as a new source of energy and electricity necessitates the development of new refractory materials resistant to harsh operating environment of black liquor gasifiers. These materials will contribute considerably in providing stable conditions for energy production with this new technology. Literature review shows that for alumino silicates at low temperatures (≤1260ºC) spalling, bloating and peeling and at higher temperatures (≥1260ºC), viscous flow is the wear mechanisms. In the case of fireclay refractories, nepheline, kalsalite and lucite are formed. In the case of alumina, Beta-alumina and sodium aluminate are formed as expansive phases. Noselite is formed at T >1150ºC in fireclay bricks due to sodium sulfate condensation. Based on thermodynamics, in contact with black liquor, alpha-alumina converts to β”-alumina, β-alumina and K-β-alumina, and mullite converts to nepheline, albite, leucite and corundum. Thermodynamic analysis based on FactSage database shows that zirconia, barium aluminate and lithium aluminate may have satisfactory stability against black liquor but alumina will be corroded. Experimental analysis is necessary to verify the result of thermodynamics. Static and dynamic immersion corrosion set-ups will show whether reaction or diffusion is the rate controlling step of corrosion process. Optical and electron microscopy with X-ray diffraction will help us to discover the corrosion mechanism of selected materials in exposure to sodium and potassium carbonate smelts.

REFERENCES

1. M. Marklund, "Black Liquor Recovery: How does it work?" (ETS), http://etcpitea.se/blg/document/PBLG_or_RB.pdf.
2. K. Whitty, University of Utah, ACERC Annual Meeting, 14-15 March, 2002.
3. L.L. Stigsson, B. Hesseborn, "Gasification of Black Liquor", Proceedings of International Chemical Recovery System, Toronto, Ontario, ppB277-295, 1995
4. J. Rudberg, Chemrec AB, Presentation at IEA ANNEX XV Semi-Annular Meeting, Atlanta, USA, February 11, 2003.
5. E.D. Larson, D. R. Raymond, "Commercialization Black Liquor and Biomass Gasifier/Gas Turbine Tecknology",Tappi Journal, Vol.80, No.12, pp50-57, 1997
6. C. A. Brown, P. Smith, "Update of North America's First Commercial Black Liquor Gasification Plant" Proceedings of Engineering & Papermakers Conference; Nashville, TN, pp33-49, 1997.
7. C. L. Verrill, "Development and Evaluation of a Low-Temperature Gasification Process for Chemical Recovery from Kraft Black Liquor", International Chemical Recovery Conference, Tampa, Florida, pp1067-1078, 1998.
8. J. R. Keiser, R. A. Peascoe and C. R. Hubbard, "Corrosion Issues in Black Liquor Gasifiers", San Diego, CA, March 16–20, 2003.
9. P. Tucker from International Paper (session leader), K. Bowers, "Closing in on Black Liquor and Biomass Gasification/Combined-Cycle", http://www.tri-inc.net/A2020BLGasification.pdf.
10. L. Stigsson, "Chemrec Black Liquor Gasification", International Chemical Recovery Conference, Tampa, Florida, pp663-674, 1998.
11. B. Aghamohammadi, "Large Scale Pilot Testing of the MTCI/Thermochem Black Liquor System Reformer", Proceedings of International Chemical Recovery System, Toronto, Ontario, Vol.B, pp297-301, 1995.
12. P. Ulmegren, R. Radestrom, "On the Chemistry of Non-Process Elements in Systems with a Pressurized Black Liquor Gasifier", International Chemical Recovery Conference, Tampa, Florida, pp721-732, 1998.
13. StoneChem, Inc, Presentation at IEA ANNEX XV Semi-Annular Meeting, Atlanta, USA, February 11, 2003.
14. C. A. Brown, "Operating Experience at North America's first Commercial Black Liquor Gasification Plant", Proceedings of International Chemistry Recovery Cconference", pp655-662 (1998).
15. S. Consonni, E. Larson and N. Berglin, "Black Liquor Gasifier/Gas Turbine Cogeneration", ASME, **97**, 1-9 (1997).
16. K. McAlister & E. Wolfe, "A Study of the Effects of Alkali Attack on Refractories Used in Incineration", Proceedings of Incineration Conference, Albuquerque, New Mexico, pp.631-638 (1992).
17. A. Yamaguchi, "Reactions between Alkaline Vapors and Refractories for Glass Tank Furnaces", Proceedings of International Congress on Glass, Kyoto, Japan, pp.1-8 (1974).
18. E. A. Thomas, "A Study of Soda and Potash Vapor Attack on Super Structure Refractories", J. Can. Ceram. Soc, 44, 37-41 (1975).

19. N. R. Brown, “Alkali Vapor Attack of Alumino-Silicate refractories”, Proceedings of International Ceramic Conference: AUSTCERAM 88, Sydney, pp.711-715, (1988).
20. C. R. Kennedy, “Alkali attack on mullite refractory in the grand forks energy technology center slagging gasifier”, Journal of Materials for Energy Systems, 3[N-1, June] 27-31, (1981).
21. B. H. Bieler, “Corrosion of AZS, Zircon and Silica Refractories by Vapors of NaOH and of Na_2CO_3”, J. Am. Ceram. Soc. Bull, 61[7], 745-749, (1982).
22. J. R. LeBlanc, ”Brockway’s Lower Checker Sulfate Test”, J. Can. Ceram. Society, 52, 58-60, (1983).
23. R. A. Peascoe, J. R. Keiser, “Performance of Selected Materials in Molten Alkali Salts”, 10th International Symposium on Corrosion in the Pulp and Paper Industry (10th ISCPPI); Marina Congress Center, Helsinki, Finland, pp189-200, 2001.
24. F. Tadaoki, “Corrosion of Zircon Refractories by Vapors of Sodium Compounds”, Ashi Gavasu Kenkya Hokoku, 17(2), 77-98 (1967).
25. J. Gullichsen, H. Paulapuro, “Chemical Pulping, Paper Making Science and Technology”, Book 6B.

BIBLIOGRAPHY

W. E. Lee, S. Zhang, "Melt Corrosion of Oxide and Oxide-Carbon Refractories", A Review from Dept. of Engineering Materials, University of Sheffield, UK., 1999.
V. G. Levich, "Physicochemical Hydrodyanamics", 1962. Englewood Cliffs, NJ, USA, Prentice-Hall.
W. D. Kingery, H. K. Bowen, D. R. Uhlmann, "Introduction to Ceramics", Second ed. , John Wiley & Sons. New York, 1976.
R. A. McCauley, "Corrosion of Ceramics", 1994, New York, Marcel Deker.
M. L. Millard, "The Effect of Microstructure on the Liquid Corrosion of Sodium Chloride and Aluminum Oxide", Ph.D. Dissertation, Department of Ceramic Engineering, University of Missouri-Rolla, 1982.
Y. Chung, "Corrosion of Partially Stabilized Zirconia by Steelmaking Slags", M.S. Thesis, Department of Ceramic Engineering, University of Missouri-Rolla, 1993.
C. Wagner, "The Dissolution Rate of Sodium Chloride with Diffusion and Natural Convection as Rate-Determining Factors", J. Phys. Colloid Chem., 53, 1030-33, 1949.
L. Reed, L. R. Barrett, "The Slagging of Refractories, I. The Controlling Mechanism in Refractory Corrosion", Trans. Brit. Ceram. Soc, 54, 671-676, 1955.
Y. Kuromitsu, H. Yoshida, "Interaction between Alumina and Binary Glasses", J. Am. Ceram. Soc, 80 [6] 1583-87, 1997.
L. Reed, L. R. Barrett, "The Slagging of Refractories, II. The Kinetics of Corrosion", Trans. Brit. Ceram. Soc. 63, 509-534, 1964.
R. Sangiorgi, "Corrosion of Ceramics by Liquid Metals", NATO ASI Ser., Ser E., Applied Sciences, Vol. 267, pp. 261-84, 1994
N. McCallum, L. R. Barrett, "Some Aspects of the Corrosion of Refractories", Trans. Brit. Ceram. Soc., 51, 523-543, 1952.
A. R. Cooper, Jr, W. D. Kingery, "Dissolution in Ceramic Systems: I, Molecular Diffusion, Natural Convection and Forced Studies of Sapphire Dissolution in Calcium Aluminum Silicate", J. Am. Ceram. Soc, 47 [1], 37- 43, 1964.
M. P. Borom, R. H. Arendt, "Dissolution of Oxides of Y, Al, Mg, and La by Molten Fluorides", Ceramic Bulletin, 60 [11], 1169-1174, 1981.
S. E. Feldman, W. K. Lu, "Kinetics of the Reactions between Silica and Alumino-Silicate Refractories and Molten Iron", Metallurgical Transactions, 5, 249-253, 1974.
B. N. Samaddar, W. D. Kingery, A. R. Cooper, "Dissolution in Ceramic Systems: II, Dissolution of Alumina, Mullite, Anorthite, and Silica in a Calcium-Aluminum-Silicate Slag", J. Am. Ceram. Soc, 47 [5] 249-254.
K. McAlister & E. Wolfe, "A Study of the Effects of Alkali Attack on Refractories Used in Incineration", Proceedings of Incineration Conference, Albuquerque, New Mexico, pp.631-638 (1992).
Yamaguchi, A, "Reactions between Alkaline Vapors and Refractories for Glass Tank Furnaces", Proceedings of International Congress on Glass, Kyoto, Japan, pp.1-8 (1974).
Thomas, Everett A, "A Study of Soda and Potash Vapor Attack on Super Structure Refractories", *J. Can. Ceram. Soc*, **44**, 37-41 (1975).
Brown, N.R. "Alkali Vapor Attack of Alumino-Silicate refractories", Proceedings of International Ceramic Conference: AUSTCERAM 88, Sydney, pp.711-715, (1988).

Kennedy, Christophere R, "Alkali attack on mullite refractory in the grand forks energy technology center slagging gasifier", *Journal of Materials for Energy Systems*, **3**[N-1, June] 27-31, (1981).
LeBlanc, John R, "Brockway's Lower Checker Sulfate Test", *J. Can. Ceram. Society*, **52**, 58-60, (1983).
Barrie H. Bieler, "Corrosion of AZS, Zircon and Silica Refractories by Vapors of NaOH and of Na_2CO_3", *J. Am. Ceram. Soc. Bull*, **61**[7], 745-749, (1982).
R. A. Peascoe, J. R. Keiser, "Performance of Selected Materials in Molten Alkali Salts", 10^{th} International Symposium on Corrosion in the Pulp and Paper Industry (10^{th} ISCPPI); Marina Congress Center, Helsinki, Finland, pp189-200, 2001.
Tadaoki Fukui, "Corrosion of Zircon Refractories by Vapors of Sodium Compounds", *Ashi Gavasu Kenkya Hokoku*, **17**(2), 77-98 (1967).
J. Gullichsen, H. Paulapuro, "Chemical Pulping, Paper Making Science and Technology", Book 6B.

LIST OF ACRONYMS AND ABBREVIATIONS

ADMT=Air Dried per Metric Ton
BL=Black Liquor
BLG=Black Liquor Gasification
LPLT=Low Pressure Low Temperature
HPLT=High Pressure Low Temperature
LPHT=Low Pressure High Temperature
HPHT=High Pressure High Temperature
MTCI=Manufacturing Technology Conversion International, Inc.
N=Na2O
A=Al2O3
S=SiO2
K=K2O
AZS=Alumina-Zirconia-Silicate
P_t=Pressure
T=Temperatura
ΔG=Change in Gibb's Free Energy

APPENDIX – SIMPLE COMPOUND TABLE

SIMPLE OXIDES

Mineral name	Formula	M. W.	m.p., C or [decomposition temperature]	density	hardness		solubility	Alfa Aesar code	cost ($)/kg powder 99.5% purity min
corundum, alfa-alumina	Al2O3	101.96	2050-2054	3.96-3.97	9		i H2O/os	12553	47
	CeO2	172.14	2400	7.65			i H2O, dil acid	40581	52 (98%)
	CoO	74.93	1830	6.44			i H2O	40184	380 (-400 mesh)
	Er2O3	382.52	2418	8.64			i H2O, s acid	11310	283 (<30 micron)
	HfO2	210.49	2774	9.68			i H2O	40270	542 (technical grade, -8 mesh)
	In2O3	277.63	1913	7.18			i H2O, s hot acid	43137	14,040 (.01-.02 micron)
	La2O3	325.81	2305	6.51			i H2O, s dil acid	11272	111
	Li2O	29.88	1570	2.013				42530	1,820 (0.1-6 mm)
periclase	MgO	40.31	2800-2826	3.56-3.6	5.5		sl H2O	43195	330 (95%, -140+325 mesh)
manganosite	MnO	70.94	1840-1850	5.37	5.5		i H2O, s acid	11870	26 (99%, +200 mesh)
	Mn3O4	228.81	1567	4.84			i H2O, s HCl	87791	65 (-325 mesh)
	Nd2O3	336.48	2272-2320	7.24			i H2O, sl dil acid	11248	268
	Sm2O3	348.72	2300-2335	7.6				11229	423
	Sc2O3	137.91	2485	3.864			s conc acid	11216	23,400
cristobalite	SiO2	60.09	1710-1720	2.334			i H2O, acid, s HF	13024	14 (-400 mesh)
	ThO2	264.04	3390-3590	9.99			i H2O, alk, sl acid	14740	5,808 (-325 mesh)
cassiterite	SnO2	150.69	1630	6.85-6.995	6.5		i H2O, s acid	12283	84 (<10 micron)
rutile	TiO2	79.87	1843-1855	4.23-4.25	6.5		2O, dil acid, s conc a	43047	42 (1-2 micron)
	WO2	215.84	[1500-1700]	10.8			i H2O, os	40387	3,360 (-100 mesh)
	WO3	231.84	1472	7.2			i H2O, sl acid, s alk	11828	190 (10-20 micron)
	UO2	270.03	2827-2900	10.97	4.5		2O, dil acid, s conc a	12106	3,465 (-100 mesh)
	VO2	82.94	1967	4.339			i H2O, sl acid, alk	22957	3,040 (-100 mesh)
	Yb2O3	394.08	2435	9.2			s dil acid	11191	349
	Y2O3	225.81	2410-2439	5.03			s dil acid	11180	137 (<10 micron)
cubic zirconia	ZrO2	123.22	2710-2715	6.205			i H2O, sl acid	11395	94 (99+%, -325 mesh)

APPENDIX – COMPLEX COMPOUND TABLE

5	COMPLEX	OXIDES										
CRC No.	Index No. Routschka's book	Mineral name	Formula	M.W.	mp, C or [decomposition temp.]	density	emmisivity	hardness	solubility	Alfa Aesar code	costikg powder 99% or higher	Phase Diagrams for Ceramists
			CaO.Al2O3	158	1600	2.98				22646	2,420 (-200 mesh)	
			Al2O3.TiO2	181.9	1860					14484	1,050 (-100 mesh)	316
			BaO.P2O5	295.3	1560				I H2O, s ac	22641	187 (90+%)	
	OXM-020	mayenite	12CaO.7Al2O3	1387	1455	2.826		5				231
	OXM-024	gehlenite	2CaO.Al2O3.2SiO2	274.2	1590	3.04						
	OXM-045	akermanite	2CaO.MgO.2SiO2	272.6	1454	3.15						
464	OXM-106		2CaO.P2O5	254.1	1353	3.1			I H2O, s dil a	89836	27 (98%)	
	OXM-026	bredigite	2CaO.SiO2	172.4	2130	3.31				39420	608 (-325 mesh)	
			2MgO.3SiO2	260.9						3336	26	
	OXM-112	Mg-PSZ	2MgO.10ZrO2	163.5	13137					12343	69 (4 micron)	
	OXM-051	alfa cordierite	2MgO.2Al2O3.5SiO2	585	[1460]			7.5				
1234	OXM-036	forsterite	2MgO.SiO2	140.7	1890	3.126		6.5	I H2O			
	OXM-100		2MgO.TiO2	160.5	1732	3.53						
1278	OXM-038	tephorite	2MnO.SiO2	202	[1345]	4.04		6	I H2O			
	OXM-018	mullite	3Al2O3.2SiO2	426.1	[1840]	3.03						
	OXM-111	PSZ	3CaO.17ZrO2	2263		5.56						
	OXM-031	rankinite	3CaO.2SiO2	268.4	[1464]							
420	OXM-019	tri-Ca aluminate	3CaO.Al2O3	270.2	[1520]							231
	OXM-055	grossular	3CaO.Al2O3.3SiO2	450.5	[1265]	3.5						
	OXM-049	merwinite	3CaO.MgO.2SiO2	328.7	[1575]	3.15		6				630
	OXM-105		3CaO.P2O5	310.2	1730							
	OXM-032	alite	3CaO.SiO2	228.3	[1900]	3.22						
	OXM-058	pyrope	3MgO.Al2O3.3SiO2	403.2	[1365]	3.51						702
	OXM-050	melilite	4CaO.Al2O3MgO.3SiO2	546.8	1390	2.95		5.5				
	OXM-104		4CaO.P2O5	366.3	[1630]							246
	OXM-054	sapphirine	4MgO.Al2O3.3SiO2	791.2	[1462]	3.45		7.5				
	OXM-061	silicocarnotite	5CaO.P2O5.SiO2	482.2	[1300]	3.06						
	OXM-062	nagelschmidite	7CaO.P2O5.2SiO2	654.7	[<1600]	3.035						
	OXM-113	Y-PSZ	8Y2O3.92ZrO2	13143		5.96						354
			Al(PO3)3	263.9	1527	2.78			I H2O			
38	OXM-014	Al phosphate	Al2O3.P2O5	243.9	>1460	2.56			I H2O, sl sol	11109	71 (98%)	
46	OXM-015	andalusite	Al2O3.SiO2	162.1		3.145		7.5				313-314
	OXM-016	kyanite	Al2O3.SiO2	162.1	[1325]	3.65		4.5-6.5				
	OXM-017	sillimanite	Al2O3.SiO2	162.1	[1545]	3.2		6.5				
209			BaAl2O4	255.3	1827							
245			BaO.Nb2O5	413.1	1465	5.44			I H2O			
266			Ba2Na(NbO3)3	1002	1437	5.4			I H2O			
244			BaO.MoO3	241	1460	4.875			I H2O	40205	1,150 (-100 mesh)	
	OXM-064	celsian	BaO.Al2O3.2SiO2	375.5	1740			6				
263			BaO.2SiO2	273.5	1420	3.7						
264			BaO.SiO2	213.4	1605	4.4			I H2O, s ac	15122	198	
261			BaO.TiO2		1620				I H2O	12348	30 (-325 mesh)	213
262			BaO.WO3	385.2		5.04			I H2O	14520	525 (-200 mesh)	
265			BaO.ZrO2	276.5	2500	5.52			I H2O, alk, sl s	14028	66 (1-2 micron)	566
	OXM-022	Ca-di aluminate	CaO.2Al2O3	260	1750	2.91		5.5				
	OXM-023	Ca hexa-aluminate	CaO.6Al2O3	667.9	[1850]	3.38						
	OXM-025	anorthite	CaO.Al2O3.2SiO2	278.2	1550	2.765		6				
	OXM-045	diopside	CaO.MgO.2SiO2	216.6	1392	3.28		5.5				
	OXM-042	monticellite	CaO.MgO.SiO2	156.5	[1498]	3.2		5.5				
	OXM-044	glaucochroite	CaO.MnO.SiO2	167.1	1355	3.407		6				
	OXM-026	beta pseudo wollastonite	CaO.SiO2	116.2	1544	2.9		5		35843	248 (-200 mesh)	
479	OXM-094	perovskite	CaO.TiO2	136	1915	4.04		5.5		11397	26 (99+%, -325 mesh)	
	OXM-095	titanite, sphene	CaO.TiO2.SiO2	196.1	1355	3.5		5.5				
	OXM-110	Calcia-zirconia	CaO.ZrO2	179.3	2550	4.76				12344	37 (-325 mesh)	
480			CaO.WO3						I H2O, s hot s	13051	202 (-325 mesh)	
	OXM-012	K beta corundum	K2O.11Al2O3	1216		3.96		9				407
	OXM-067	kalsilite	K2O.Al2O3.4SiO2	436.5	1686	2.47		6				
			LiAlO2	65.92	>1625	2.62				13412	94 (-100 mesh)	
	OXM-085	high eukryptite	Li2O.Al2O3.2SiO2	252	[1400]	2.31		6				
	OXM-087	high spodumene	Li2O.Al2O3.4SiO2	372.2	1421	2.406						
1174			Li2O.MoO									
			Li2TiO3	109.8	1520-1564					13411	100	
	OXM-102	kamaolite	MgO.2TiO2	200.1	1652	3.63						
	OXM-001	spinel	MgO.Al2O3	142.3	2135	3.55				22950	182 (99%, -325 mesh)	
1233	OXM-039	enstatite, pyroxene	MgO.SiO2	100.4	[1560]	3.175		5.5				
1245	OXM-101	geikielite	MgO.TiO2	120.2	1610-1630	3.895				11398	45 (2 micron)	
1247			MgWO4	272.1	1246	7.3			s dil ac	14023	,080 (99%, -325 mesh)	
			MgO.Al2O3.ZrO2	265.5						36368	2,030 (99%, 3-12 mm)	
	OXM-007	galaxite	MnO.Al2O3	172.9	[1560]	4.23						275
1289	OXM-009	hausmannite	MnO.Mn2O3	228.8	1562	4.84		5.5	I H2O, HCl			
1287	OXM-097	pyrophanite	MnO.TiO2	150.8	[1360]	4.57				13133	3,620 (-100 mesh)	277
	OXM-013	Na beta corundum	Na2O.11Al2O3	1164	1565	3.96		9				
			Na2O.3TiO2	301.7	1551					14137	86 (98+%, -325 mesh)	
1983			SrO.TiO2	183.5	2080	4.81				11389	60 (99+%)	297
	OXM-010	gahnite	ZnO.Al2O3	183.3	1950	4.607		8				
2298			Y3Al5O12	593.6	1970	~4.5						311
2378	OXM-114	zircon	ZrO2.SiO2	183.3	[1775]	4.68		7.5				
	OXM-092		4CaO.3TiO2	464	[1755]							240
	OXM-093		3CaO.2TiO2	328	[1740]	3.55		5.5				

APPENDIX – PHASE DIAGRAMS

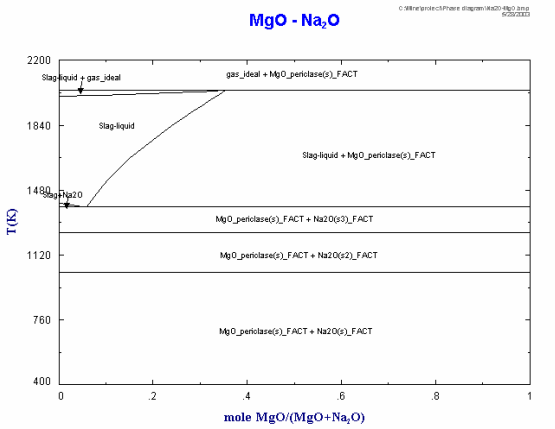

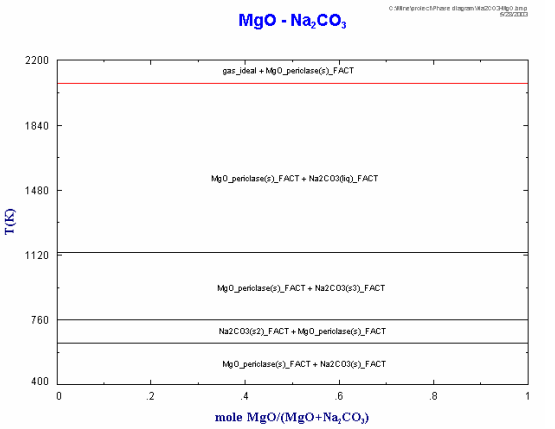

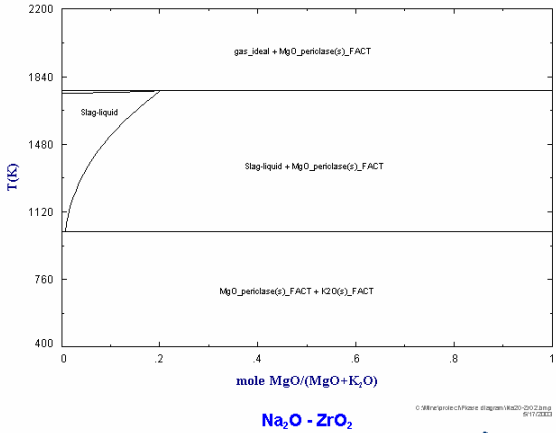

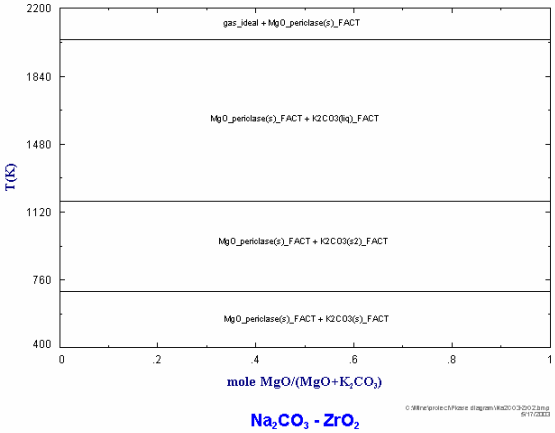

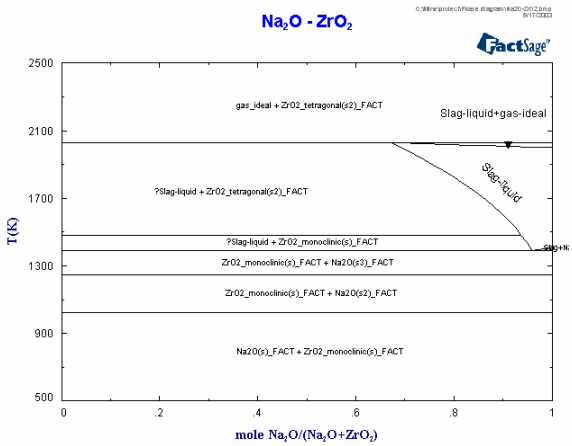

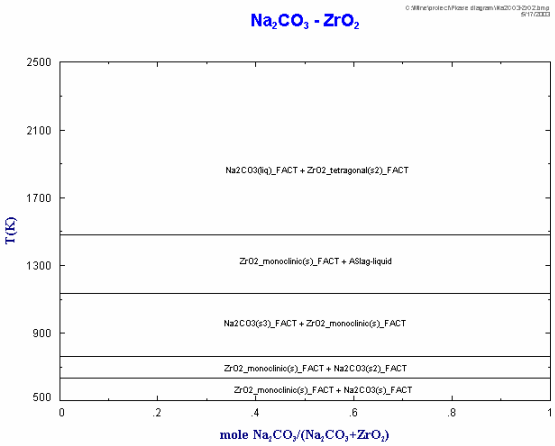

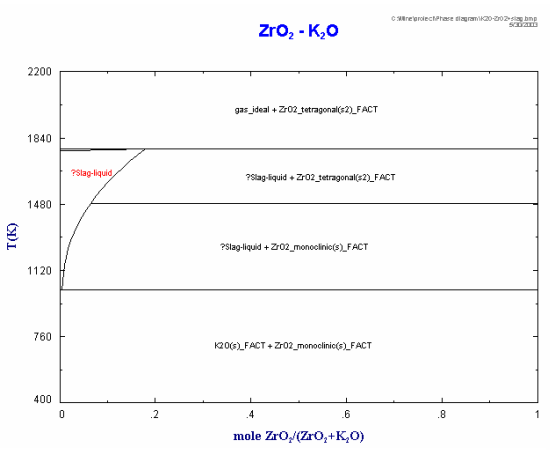
ZrO2 - K2O
gas_ideal + ZrO2_tetragonal(s2)_FACT
?Slag-liquid
?Slag-liquid + ZrO2_tetragonal(s2)_FACT
?Slag-liquid + ZrO2_monoclinic(s)_FACT
K2O(s)_FACT + ZrO2_monoclinic(s)_FACT
T(K)
mole ZrO2/(ZrO2+K2O)

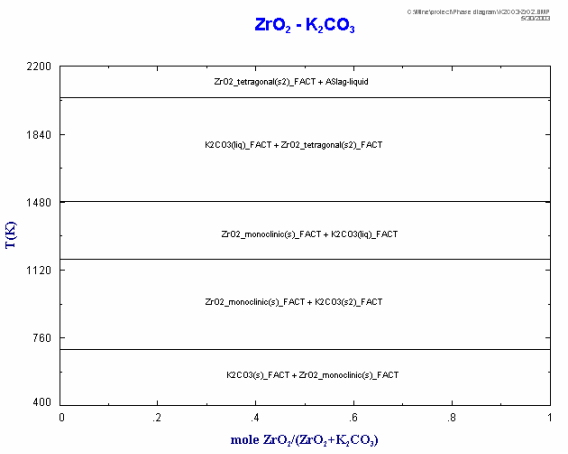
ZrO2 - K2CO3
ZrO2_tetragonal(s2)_FACT + ASlag-liquid
K2CO3(liq)_FACT + ZrO2_tetragonal(s2)_FACT
ZrO2_monoclinic(s)_FACT + K2CO3(liq)_FACT
ZrO2_monoclinic(s)_FACT + K2CO3(s2)_FACT
K2CO3(s)_FACT + ZrO2_monoclinic(s)_FACT
T(K)
mole ZrO2/(ZrO2+K2CO3)

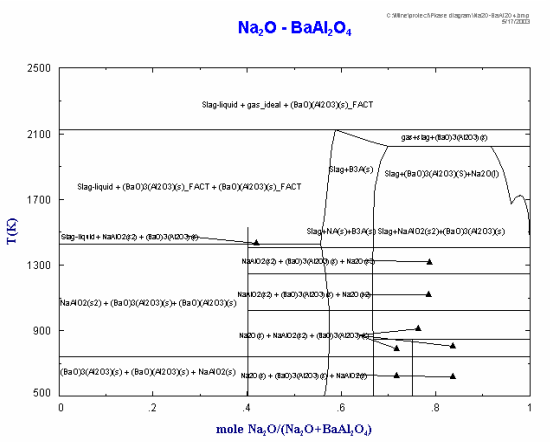
Na2O - BaAl2O4
Slag-liquid + gas_ideal + (BaO)(Al2O3)(s)_FACT
Slag-liquid + (BaO)3(Al2O3)(s)_FACT + (BaO)(Al2O3)(s)_FACT
NaAlO2(s2) + (BaO)3(Al2O3)(s)+ (BaO)(Al2O3)(s)
(BaO)3(Al2O3)(s) + (BaO)(Al2O3)(s) + NaAlO2(s)
T(K)
mole Na2O/(Na2O+BaAl2O4)

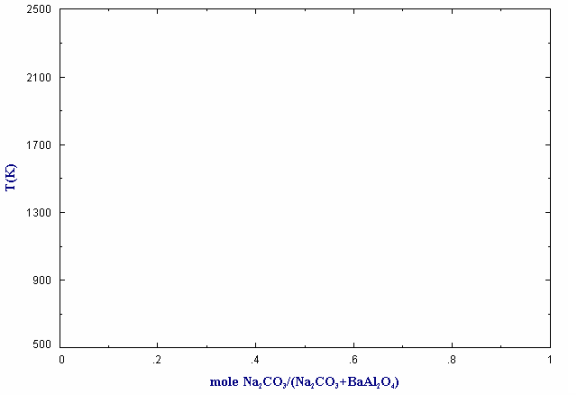
Na2CO3 - BaAl2O4
T(K)
mole Na2CO3/(Na2CO3+BaAl2O4)

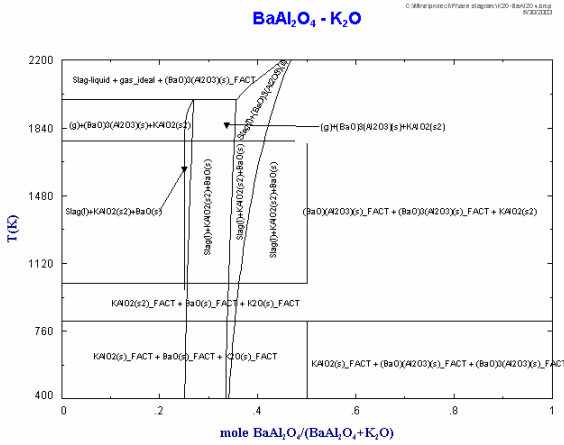
BaAl2O4 - K2O
Slag-liquid + gas_ideal + (BaO)(Al2O3)(s)_FACT
(g)+(BaO)(Al2O3)(s)+KAlO2(s2)
(g)+(BaO)(Al2O3)(s)+KAlO2(s2)
Slag()+KAlO2(s2)+BaO(s)
(BaO)(Al2O3)(s)_FACT + (BaO)3(Al2O3)(s)_FACT + KAlO2(s2)
KAlO2(s2)_FACT + BaO(s)_FACT + K2O(s)_FACT
KAlO2(s)_FACT + BaO(s)_FACT + K2O(s)_FACT
KAlO2(s)_FACT + (BaO)(Al2O3)(s)_FACT + (BaO)3(Al2O3)(s)_FACT
T(K)
mole BaAl2O4/(BaAl2O4+K2O)

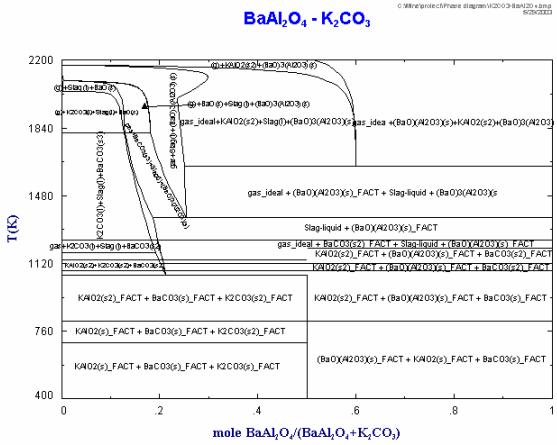
BaAl2O4 - K2CO3
gas_ideal + (BaO)(Al2O3)(s)_FACT + Slag-liquid + (BaO)3(Al2O3)(s
Slag-liquid + (BaO)(Al2O3)(s)_FACT
gas_ideal + BaCO3(s2)_FACT + Slag-liquid + (BaO)(Al2O3)(s)_FACT
KAlO2(s2)_FACT + (BaO)(Al2O3)(s)_FACT + BaCO3(s2)_FACT
KAlO2(s2)_FACT + BaCO3(s)_FACT + K2CO3(s2)_FACT
KAlO2(s2)_FACT + (BaO)(Al2O3)(s)_FACT + BaCO3(s)_FACT
KAlO2(s)_FACT + BaCO3(s)_FACT + K2CO3(s2)_FACT
KAlO2(s)_FACT + BaCO3(s)_FACT + K2CO3(s)_FACT
(BaO)(Al2O3)(s)_FACT + KAlO2(s)_FACT + BaCO3(s)_FACT
T(K)
mole BaAl2O4/(BaAl2O4+K2CO3)

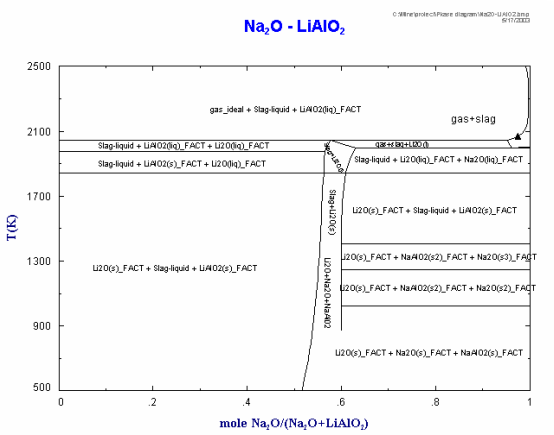
Na2O - LiAlO2
gas_ideal + Slag-liquid + LiAlO2(liq)_FACT
gas+slag
Slag-liquid + LiAlO2(liq)_FACT + Li2O(liq)_FACT
Slag-liquid + LiAlO2(s)_FACT + Li2O(liq)_FACT
Slag-liquid + Li2O(liq)_FACT + Na2O(liq)_FACT
Li2O(s)_FACT + Slag-liquid + LiAlO2(s)_FACT
Li2O(s)_FACT + NaAlO2(s2)_FACT + Na2O(s3)_FACT
Li2O(s)_FACT + NaAlO2(s2)_FACT + Na2O(s2)_FACT
Li2O(s)_FACT + Na2O(s)_FACT + NaAlO2(s)_FACT
T(K)
mole Na2O/(Na2O+LiAlO2)

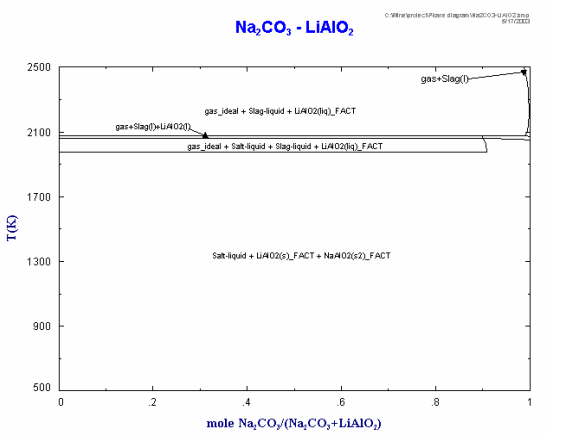
Na2CO3 - LiAlO2
gas+Slag(l)
gas_ideal + Slag-liquid + LiAlO2(liq)_FACT
gas+Slag(l)+LiAlO2(s)
gas_ideal + Salt-liquid + Slag-liquid + LiAlO2(liq)_FACT
Salt-liquid + LiAlO2(s)_FACT + NaAlO2(s2)_FACT
T(K)
mole Na2CO3/(Na2CO3+LiAlO2)

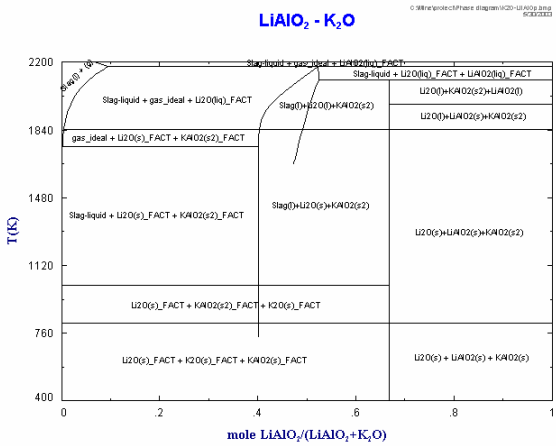
LiAlO2 - K2O
Slag-liquid + gas_ideal + Li2O(liq)_FACT + LiAlO2(liq)_FACT
Slag-liquid + Li2O(liq)_FACT + LiAlO2(liq)_FACT
Li2O(l)+KAlO2(s2)+LiAlO2(l)
Slag(l)+Li2O(l)+KAlO2(s2)
Li2O(l)+LiAlO2(s)+KAlO2(s2)
gas_ideal + Li2O(s)_FACT + KAlO2(s2)_FACT
Slag-liquid + Li2O(s)_FACT + KAlO2(s2)_FACT
Slag(l)+Li2O(s)+KAlO2(s2)
Li2O(s)+LiAlO2(s)+KAlO2(s2)
Li2O(s)_FACT + KAlO2(s2)_FACT + K2O(s)_FACT
Li2O(s)_FACT + K2O(s)_FACT + KAlO2(s)_FACT
Li2O(s) + LiAlO2(s) + KAlO2(s)
T(K)
mole LiAlO2/(LiAlO2+K2O)

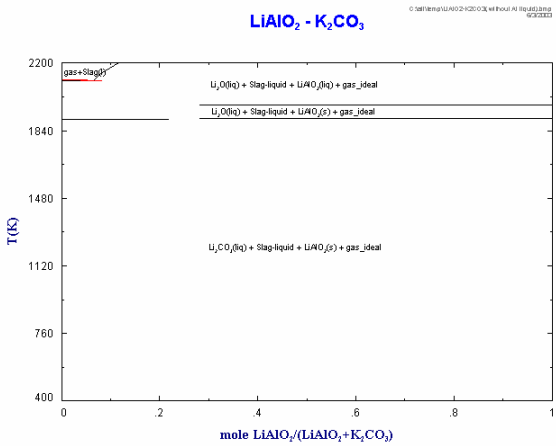
LiAlO2 - K2CO3
gas+Slag(l)
Li2O(liq) + Slag-liquid + LiAlO2(liq) + gas_ideal
Li2O(liq) + Slag-liquid + LiAlO2(s) + gas_ideal
Li2CO3(liq) + Slag-liquid + LiAlO2(s) + gas_ideal
T(K)
mole LiAlO2/(LiAlO2+K2CO3)

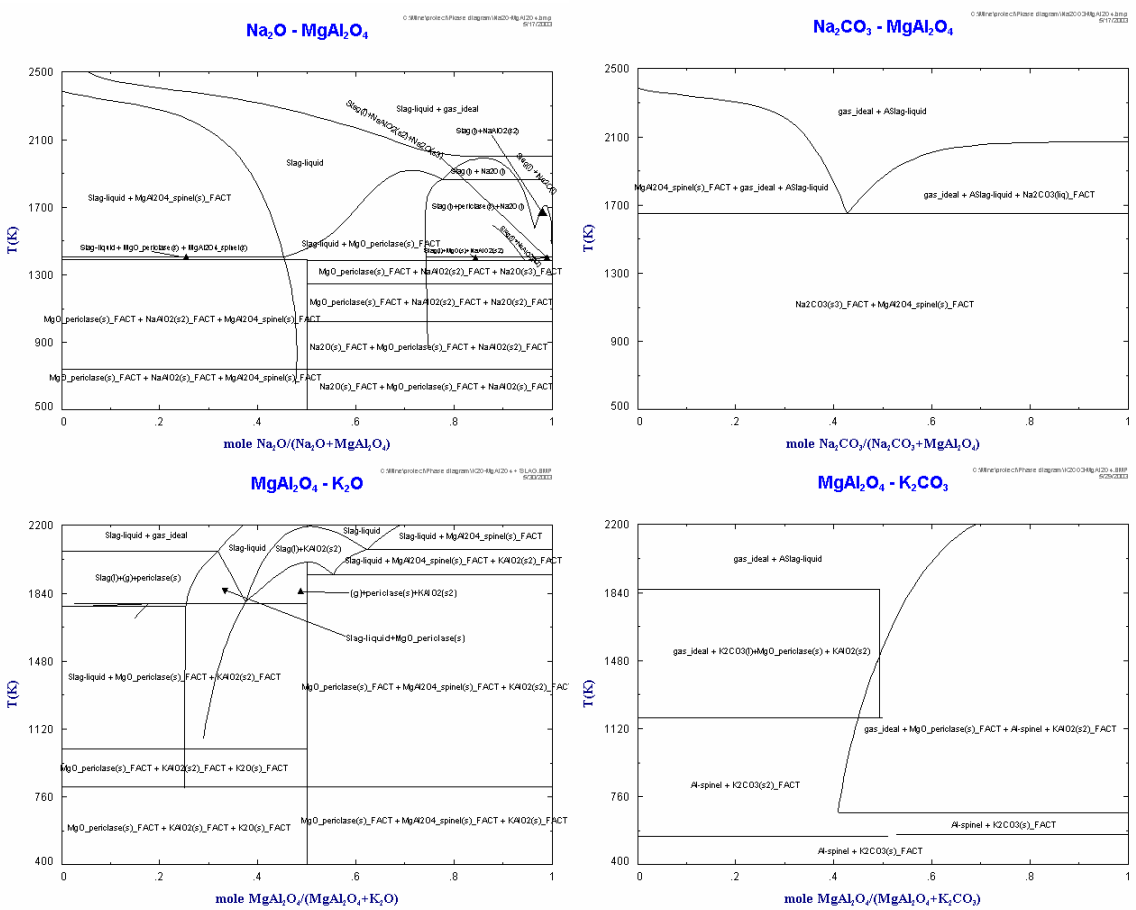
Na2O - MgAl2O4
T(K)
mole Na2O/(Na2O+MgAl2O4)
Slag-liquid + gas_ideal
Slag-liquid
Slag-liquid + MgAl2O4_spinel(s)_FACT
Slag-liquid + MgO_periclase(s)_FACT
MgO_periclase(s)_FACT + NaAlO2(s2)_FACT + Na2O(s3)_FACT
MgO_periclase(s)_FACT + NaAlO2(s2)_FACT + Na2O(s2)_FACT
MgO_periclase(s)_FACT + NaAlO2(s2)_FACT + MgAl2O4_spinel(s)_FACT
Na2O(s)_FACT + MgO_periclase(s)_FACT + NaAlO2(s2)_FACT
MgO_periclase(s)_FACT + NaAlO2(s)_FACT + MgAl2O4_spinel(s)_FACT
Na2O(s)_FACT + MgO_periclase(s)_FACT + NaAlO2(s)_FACT
Na2CO3 - MgAl2O4
T(K)
mole Na2CO3/(Na2CO3+MgAl2O4)
gas_ideal + AStag-liquid
MgAl2O4_spinel(s)_FACT + gas_ideal + AStag-liquid
gas_ideal + AStag-liquid + Na2CO3(liq)_FACT
Na2CO3(s3)_FACT + MgAl2O4_spinel(s)_FACT
MgAl2O4 - K2O
T(K)
mole MgAl2O4/(MgAl2O4+K2O)
Slag-liquid + gas_ideal
Slag-liquid
Slag-liquid + MgAl2O4_spinel(s)_FACT
Slag-liquid + MgAl2O4_spinel(s)_FACT + KAlO2(s2)_FACT
Slag-liquid+MgO_periclase(s)
Slag-liquid + MgO_periclase(s)_FACT + KAlO2(s2)_FACT
MgO_periclase(s)_FACT + MgAl2O4_spinel(s)_FACT + KAlO2(s2)_FACT
MgO_periclase(s)_FACT + KAlO2(s2)_FACT + K2O(s)_FACT
MgO_periclase(s)_FACT + KAlO2(s)_FACT + K2O(s)_FACT
MgO_periclase(s)_FACT + MgAl2O4_spinel(s)_FACT + KAlO2(s)_FACT
MgAl2O4 - K2CO3
T(K)
mole MgAl2O4/(MgAl2O4+K2CO3)
gas_ideal + AStag-liquid
gas_ideal + K2CO3(l)+MgO_periclase(s) + KAlO2(s2)
gas_ideal + MgO_periclase(s)_FACT + Al-spinel + KAlO2(s2)_FACT
Al-spinel + K2CO3(s2)_FACT
Al-spinel + K2CO3(s)_FACT
Al-spinel + K2CO3(s)_FACT